HHS Public Access

An intra-amygdala circuit specifically regulates social fear learning

Robert C. Twining[*], **Jaime E. Vantrease**[*], **Skyelar Love**, **Mallika Padival**, and **J. Amiel Rosenkranz**

Department of Cellular and Molecular Pharmacology, The Chicago Medical School, Rosalind Franklin University of Medicine and Science, 3333 Green Bay Road, North Chicago, Illinois USA

Abstract

Adaptive social behavior requires transmission and reception of salient social information. Impairment of this reciprocity is a cardinal symptom of autism. The amygdala is a critical mediator of social behavior and is implicated in social symptoms of autism. Here we found that a specific amygdala circuit, from the lateral nucleus to the medial nucleus (LA-MeA), is required for using social cues to learn about environmental cues that signal imminent threats. Disruption of the LA-MeA circuit impaired valuation of these environmental cues and subsequent ability to use this cue to guide behavior. Rats with impaired social guidance of behavior due to knockout of *Nrxn1*, an analog to autism-associated genes (*NRXN*), exhibited marked LA-MeA deficits. Chemogenetic activation of this circuit reversed these impaired social behaviors. These findings identify an amygdala circuit required to guide emotional responses to socially significant cues and identify a novel exploratory target for disorders associated with social impairments.

The reciprocal exchange of information by social interaction is a key ability that promotes survival. This ability allows an observer to deduce the intentions and emotions of others by interpretation of social cues, such as facial expression and body posture. One consequence is a capacity to avoid threats by observing the association between others' social cues and co-occurring events. Previous studies have implicated several interconnected brain regions as a social network that contributes to the transmission and reception of social information. The amygdala is a key component of this network[1–5], and may serve as a link between

recognition of social cues and the production of socially-motivated affective responses. In support of this, the amygdala displays functional abnormalities in individuals with impaired social comprehension, such as people with autism[6,7].

The nuclei of the amygdala work together to orchestrate a range of affective behaviors. However, intra-amygdala connections that guide learned social behavior are not known. The lateral nucleus (LA) of the basolateral complex is implicated in guidance of affective behavior by environmental cues. Outputs from the LA to the central amygdala, bed nucleus of stria terminalis and nucleus accumbens guide autonomic and behavioral aspects of fear and appetitive behavior in response to learned cues[8–10]. The posterior medial amygdala (MeA) also receives input from the LA[11], is an essential mediator of social behavior[4,12–15] and exhibits patterns of activation consistent with a role in social learning[16]. Therefore, interaction between LA and MeA might be required for successfully linking social cues with an appropriate learned affective response. There is little iknown about the LA and MeA interaction or how their interaction may be impaired in aberrant social comprehension.

The purpose of this study was to test the importance of the LA-MeA circuit in social behaviors, and to identify whether the LA-MeA path can serve as a link between comprehension of a social behavior and appropriately using that information to guide behavior.

Results

Amygdala circuit in social learning

To test whether the LA-MeA path can serve as a link between comprehension of a social behavior and the appropriate use of that information to guide responses, we employed a social fear conditioning paradigm. The premise of this approach is that a rat that values social cues produced by a conspecific can use those cues to guide their immediate affective behavior, and can also imbue associated environmental cues and contexts with affective significance. The valuation of social cues can be inferred from the use of associated conditioned cues and contexts to guide behavior. In social fear conditioning, a 'demonstrator' undergoes classical fear conditioning (foot shock paired with conditioned stimulus (CS+)) with a conspecific 'observer' in close proximity[17]. In these experiments, rats are separated only by a mesh barrier[18] (Figure 1a). The behavior of these rats is measured over the entire course of fear conditioning and again in response to the CS+ after 48 hours. An appropriate affective response to the CS+ in this task requires the observer rat to successfully recognize and process a social cue and associate this social cue with environmental cues. Observer rats readily demonstrated social approach (Figure 1b) during initial phases of this task and developed freezing in response to the CS+ tone (Figure 1c), despite no direct experience with foot shock. When tested after 48 hours, observer rats exhibited contextual freezing in the same chamber (Figure 1d) and cued freezing to the CS+ in a novel chamber (Figure 1e). To verify that this was a result of social transmission this same conditioning paradigm was repeated with an anesthetized demonstrator. When conditioning was performed with an anesthetized demonstrator, the observing rat displayed less approach behavior (Figure 1b; eta^2=0.25, 95% C.I.=−26.8 to −2.5; eta^2=0.29, 95% C.I.= −35.9 to −4.9, two-tailed unpaired t-test;), did not display freezing during conditioning

(Figure 1c; eta^2=0.10, one-way RM-ANOVA) and less conditioned freezing during contextual and cued testing (Figure 1d,e; eta^2=0.35, 95% C.I.=5.94 to 28.0, two-tailed unpaired t-test; eta^2=0.21, two-way RM-ANOVA). This is similar to the absence of social fear conditioning if the demonstrator received no foot shock ("Tone only" control[18]). This indicates that social cues emitted by the demonstrator drive the social learning. To determine whether the MeA or LA are required for social fear learning, nuclei were bilaterally inactivated during social fear conditioning using a chemogenetic approach (AAV-CaMKIIa-HA-hM4D(Gi)-IRES-mCitrine (DREADD-Gi)[19,20]; 1 mg/kg CNO, i.p. 40 m before conditioning; Figure 2a,b). Control rats had reporter without DREADD-Gi (AAV-CaMKIIa-YFP; n=8). CNO was administered to control and DREADD-expressing rats. CNO administration decreased the activity of MeA or LA neurons in DREADD-Gi-expressing rats, but not in control rats (Figure 2c–f; eta^2=0.23, 95% C.I.=−2.9 to −1.2; eta^2=0.27, 95% C.I.=−0.69 to −0.22, two-tailed unpaired t-test), and this effect was specific for the targeted region (Figure 2g). This demonstrates the utility of this chemogenetic approach to decrease LA and MeA activity. DREADD expression and recording loci were confirmed to lie within the MeA or LA (Supplementary Figure 1 and 2). Inactivation of the LA during social fear conditioning had no effect on social approach behavior (Figure 3a), but attenuated freezing during social fear conditioning (Figure 3b; eta^2=0.11, two-way RM-ANOVA). When tested in a novel context after 48 hours, conditioned freezing to the CS+ was attenuated (Figure 3d; eta^2=0.18, two-way RM-ANOVA) while freezing to the original context in the absence of the CS+ was spared (Figure 3c). The LA, then, is a key mediator of learning to associate an environmental cue (but not context) with a paired social cue, leading to a deficit in conditioned responding to that environmental cue when tested later. To test whether the MeA is similarly required for social fear learning, MeA (posterior) was bilaterally inactivated during social fear conditioning by the same DREADD-based approach. Observer rats with MeA inactivation during social fear conditioning exhibited both reduced social approach (Figure 3a; eta^2=0.33, eta^2=0.35, one-way ANOVA) and reduced freezing in response to the conspecific that received foot shocks during conditioning (Figure 3b). When tested after 48 hours, prior MeA inactivation reduced conditioned freezing to both the CS+ and the context (Figure 3c,d; eta^2=0.36, one-way ANOVA). This is consistent with a role for the MeA in general recognition of social cues or responding to social cues. Overall, this demonstrates a specific role for LA in social learning about an important cue, and an additional, more general role for the MeA in social approach and freezing responses to conspecific foot shock during social fear conditioning.

To determine the precise role of the LA-MeA connection in social fear learning, a functional disconnection approach was utilized whereby the LA in one hemisphere and the MeA in the other hemisphere were chemogenetically inactivated during social fear conditioning (Figure 2b; functional disconnection by inactivation instead of anatomical disconnection). This approach allows for one fully functional LA and MeA to send and receive information from other brain structures during this task. The LA-MeA functional disconnection did not decrease social approach during social fear conditioning (Figure 3e), demonstrating that the LA-MeA connection is not required for normal social approach, nor recognition or responding to social cues per se. Despite normal social approach behavior, the LA-MeA functional disconnection caused reduced freezing in the observer rats to the CS+ tone over

the course of conditioning (Figure 3f; eta^2=0.047, two-way RM-ANOVA), consistent with decreased association of the CS+ tone with conspecific social cues. When tested after 48 hours, rats with prior LA-MeA functional disconnection displayed impaired freezing to the CS+ (Figure 3h; eta^2=0.22, two-way RM-ANOVA) but not contextual freezing (Figure 3g), which indicates impaired ability to learn the association between an environmental cue that is paired with a social cue. This recapitulates the effect of either bilateral LA inactivation or bilateral MeA inactivation. Inactivation of LA and MeA within one hemisphere, leaving a functional LA-MeA connection in the other hemisphere, did not significantly impair social fear conditioning (Figure 3f–h). This demonstrates that at least one functional connection between the LA and MeA is necessary and sufficient for social fear learning. The importance of the direct LA-MeA connection was further verified by selective inactivation of LA neurons that project to the posterior MeA. This was accomplished by an intersectional approach with MeA infusion of retrogradely transported viral vector that transduces expression of Cre (CAV2-Cre) and LA infusion of Cre-dependent DREADD-Gi (AAV-hSyn-DIO-hM4D(Gi)-mCherry), leading to specific expression of DREADD-Gi only in those LA neurons that project to MeA. Similar to disconnection experiments above, inactivation of the LA-MeA circuit impaired social fear conditioning (Figure 3i,j and Supplementary Figure 3; eta^2=0.16, two-way RM-ANOVA). Off-target infusions did not impair social fear conditioning (Figure 3j–l). Thus, disruption of the LA-MeA pathway (caused by bilateral inactivation of either node, functional disconnection or specific inactivation) results in a failure to use social information to imbue predictive environmental cues with emotional salience.

The specificity of the LA-MeA path in social learning of paired cues is demonstrated by intact social learning of contextual fear, which indicates that (a) the LA-MeA path is not required for the ability to freeze and form other associations based on social information, (b) the LA-MeA path is not required for recognition of social cues, and (c) the LA-MeA path is needed to link social cues with environmental cues, and to use those environmental cues to guide social behavior during conditioning. This is also consistent with other studies that demonstrate that cue-specific information is processed by the LA, while context-specific information may be processed by the basolateral nucleus of the amygdala (BA)[9]. Indeed, in experiments that included inactivation of BA-MeA path, social learning of contextual fear was impaired (Figure 3k).

To determine the specificity of the LA and MeA functional connectivity to social fear learning, we tested their role in mediating the association between a non-social aversive outcome and a neutral sensory cue in classical fear conditioning. Bilateral inactivation of the LA during classical (non-social) fear conditioning impaired conditioned freezing to a CS+ (Supplementary Figure 4a; eta^2=0.27, two-way RM-ANOVA), consistent with prior studies[9,21], and supporting the effectiveness of inactivation by DREADD-Gi. However, bilateral inactivation of the MeA or LA-MeA disconnection during classical fear conditioning did not impair conditioned freezing in response to a CS+ (Supplementary Figure 4b). Thus, the LA-MeA connection is selectively required for social fear learning, but not non-social associative learning.

The LA-MeA path may be necessary for other behaviors that contribute to social fear learning. To determine the specificity of this path's role in social fear learning, non-learned social interaction with a novel rat in an open field was measured. There was no gross abnormality in total time interacting or number of interactions upon bilateral LA or MeA inactivation or LA-MeA ipsilateral or crossed inactivation (Supplementary Figure 5a–d). A decrease in the duration of interaction events was observed upon bilateral MeA inactivation (Supplementary Figure 5b; eta^2=0.39, one-way ANOVA). This indicates that the LA-MeA path itself is not required to drive spontaneous unlearned social exploration, but the MeA contributes to sustained social interaction. No abnormalities in exploration of the open field or elevated plus maze were observed with any of the inactivation conditions (Supplementary Figure 5e,f), demonstrating that general, unconditioned anxiety behaviors are unlikely to rely on this circuit.

To further link the LA-MeA pathway with learned fear, the strength of this pathway was measured in vivo after a modified social fear learning procedure. In this modified social fear learning procedure, fewer CS+ trials were performed (3 trials, Figure 4a), to produce greater inter-individual variability in social learning. This resulted in a wider range of conditioned freezing responses to the CS+, including "bad learners" that displayed little detected conditioned freezing to the CS+ during an abbreviated test session (3 trials, <15% time freezing) and "good learners" that displayed conditioned freezing during this test session (>15% time freezing; Figure 4a). The in vivo strength of the LA-MeA path was measured in "good learners" and "bad learners" by recording the posterior MeA local field potential response upon stimulation of the LA in anesthetized rats (1.5 g/kg urethane). The input-output curve the MeA response to LA was quantified (Figure 4b). There was a significant correlation between the strength of the LA-MeA path and the amount of socially conditioned freezing to the CS+ (Figure 4c). As a control, we measured the strength of the LA-MeA path after a weak classical fear conditioning procedure (2 trials, 0.3 mA) that produced variability in non-social conditioned freezing. There was no significant association between classical conditioned freezing (3 trials) and the strength of the LA-MeA path (Figure 4c). Taken together, these data demonstrate the necessity of the LA-MeA path in the ability to use social cues to assign value to an environmental cue that predicts threat, and importantly, this ability scales as a function of the strength of the pathway.

The LA-MeA circuit in a condition with impaired social behavior

The acute deficits in responding to social cues and assigning value to socially relevant cues that was produced by inactivation of nodes in the LA-MeA circuitry is reminiscent of social deficits observed in many patients with autism. Impaired function of the LA-MeA path may contribute to social deficits in this and other disorders. Indeed, imaging studies demonstrate hyper- or hypoactivity of the amygdala associated with abnormal social behavior in autism[22,23]. The next goal of this study was to test whether a dysfunction of the LA-MeA path could underlie deficits in an animal that displays impaired social learning. Deletions and copy number variations of the neurexin gene (*NRXN*) and mutations of the neuroligin gene (*NLGN*) that encode its binding partner, are associated with autism[24,25] and neurexin has an important role in neurotransmission is several brain regions[26], leading to the expectation of abnormal social behavior in rodents with neurexin mutations. We therefore

tested if LA-MeA circuitry is impaired in rats with a knock-out of the neurexin 1 gene (*Nrxn1*) that impairs production of neurexin 1 alpha (Nrxn rats), and if this is associated with a deficit in social learning. Nrxn knockout rats[27] were bred from homozygous pairs. Age-matched WT rats of the same genetic background were bred at the same facility, housed on the same rack/room and shipped at the same time. As expected, Nrxn rats expressed significantly lower neurexin 1 mRNA and protein levels compared to WT controls (Supplemental Figure 6a,b; eta^2=0.78, 95% C.I.=−1.23 to −0.44; eta^2=0.90, 95% C.I.=−1.21 to −0.65, two-tailed unpaired t-test).

In vivo measurement of the LA-MeA connection in Nrxn rats revealed critical impairments that are consistent with those that explain aberrant responses to conspecific behavior observed in chemogenetic experiments (above). MeA activity was recorded in anesthetized rats (urethane, 1.5 g/kg) while LA was activated by a stimulation electrode. Activation of the LA evoked rapid responses in MeA of WT rats (Figure 5a, Supplementary Figure 7a–c). This response had all the characteristics of a monosynaptic input instead of antidromic or polysynaptic (latency jitter > 0.5 ms and < 3 ms, <2 ms shift in latency with increasing stimulation intensity, evoked action potentials did not display collision with pre-occurring spontaneous action potentials). The reciprocal in vivo LA activity was also measured while the MeA was stimulated in anesthetized rats. The strength of the LA-MeA path was measured as the probability of MeA neuron firing in response to LA stimulation, and was significantly stronger than the relatively weak reciprocal MeA-LA path (Supplementary Figure 7b,c) indicating that the flow of information in the LA-to-MeA direction is more efficacious. The in vivo response of MeA neurons to LA input was attenuated in Nrxn rats (Figure 5b–d), whether measured as MeA neuronal response probability or MeA local field potential response. Moreover, spontaneous firing of MeA neurons in Nrxn rats was significantly reduced compared to WT (Figure 5e; measured in vivo from anesthetized rats; eta^2=0.12, 95% C.I. −5.82 to −1.67). These data point to a deficit in LA-to-MeA transmission and a more global MeA deficit that impacts firing activity. To test the proximal basis for the impaired responsiveness of MeA neurons, membrane excitability and synaptic drive were measured *in vitro*. The neuronal excitability of MeA neurons was significantly impaired in Nrxn rats (Figure 6a; eta^2=0.21, two-way RM-ANOVA), measured as action potential firing. This was associated with significantly decreased MeA postsynaptic neuronal membrane responsiveness (input resistance, Figure 6b; eta^2=0.30, 95% C.I.=−112.2 to −35.1, two-tailed t-test), with no apparent difference in resting membrane potential (Figure 6c). There was also a significant difference in paired pulse facilitation and the coefficient of variance of glutamatergic input evoked by local stimulation (Figure 6d; eta^2=0.26, 95% C.I.=−0.60 to −0.07; eta^2=0.17, 95% C.I.=0.012 to 0.065, two-tailed t-test), an indication of reduced presynaptic reliability of excitatory synaptic input. There was little difference in spontaneous excitatory postsynaptic currents (miniature EPSCs; Figure 6e,f), perhaps because spontaneous EPSCs are induced by different presynaptic mechanisms than EPSCs evoked by action potentials [28,29]. Overall these results demonstrate that the LA-MeA circuit is impaired in Nrxn rats due to reduced input strength and attenuated responsiveness of MeA neurons. In contrast, LA neuron responsiveness was not significantly different in Nrxn rats despite similar abnormality of synaptic function (Supplementary Figure 8a–e).

To test whether the weakness in the LA-MeA connection in Nrxn rats is associated with similar outcomes as LA-MeA disconnection, we measured social behaviors. Gross social interaction behaviors and social preferences of neurexin knock-out mice have been found to be fairly normal in some studies[30] but abnormal in others[31]. Social interaction with a novel WT rat was measured to assess whether Nrxn rats demonstrate preference for social interaction. Nrxn rats did not display significant abnormality in the frequency or total time of social interactions with a novel rat (Figure 7a). However, there was a significant decrease in the duration of each social interaction (Figure 7a; eta^2=0.39, 95% C.I.=−1.36 to −0.50, two-tailed t-test), similar to the previous result we observed in the bilateral MeA-inactivated animals. There was no difference in exploration of a novel object between WT and Nrxn rats (Figure 7b). However, when given the choice between social interaction with a novel rat or exploration of a novel object, Nrxn rats displayed a significantly diminished preference for the novel rat (Figure 7c; eta^2=0.20, 95%C.I.=−1.44 to −0.22, two-tailed unpaired t-test). Taken together, this is consistent with relatively low significance of social interaction for Nrxn rats. To test the ability of Nrxn rats to learn by social transmission, we measured social fear conditioning. The Nrxn rats displayed significantly reduced approach towards the conspecific during social fear conditioning (Figure 7d; eta^2=0.35, 95% C.I.=−25.4 to −7.4; eta^2=0.49, 95% C.I.=−36.3 to −15.1, two-tailed unpaired t-test), and significantly smaller responses to the socially conditioned CS+ (Figure 7e; eta^2=0.18, two-way RM-ANOVA). This was associated with reduced conditioned freezing to the CS+ cue and context after 48 hours, consistent with impaired MeA function, including impaired guidance of MeA by LA (Figure 7f,g; eta^2=0.33, 95% C.I.=−24.2 to −6.5, two-tailed unpaired t-test; eta^2=0.13, two-way RM-ANOVA). This reduced social engagement and learning does not appear to be due to differences in the behavior of the demonstrators, which displayed similar freezing and social interactive behavior regardless of observer genotype (Supplementary Figure 9a). Previous studies demonstrate that social fear transmission can utilize auditory and olfactory components[32–34]. Nrxn rats displayed normal freezing to a loud unconditioned tone (95 dB, 1.5 kHz, 1s; Supplementary Figure 9b), indicative of unimpaired hearing ability. Nrxn rats also displayed normal ability to locate grape-flavored sucrose pellets that were buried in bedding (Supplementary Figure 9c) and discrimination between male and female pheromones, as demonstrated by time exploring used bedding from female and male rats (Supplementary Figure 9d), though they demonstrate less preference for the bedding from female rats (eta^2=0.26, 95% C.I.=1.09 to −0.02, two-tailed unpaired t-test). Overall, this is consistent with intact olfaction. However, this does not completely rule out more subtle forms of sensory deficits, and does not conclusively demonstrate the functionality of these modalities in the transfer of social information. Nevertheless, Nrxn rats displayed normal or enhanced classical fear conditioning with similar footshock sensitivity (Supplementary Figure 9e–g, consistent with a previous study[27]). Together, these data indicate that Nrxn rats exhibit hearing and olfactory function, and have the ability to learn in associative tasks that utilize an auditory CS+, yet still do not adequately use social cues to direct learning behavior. Further evidence for abnormal social processing was observed during social interaction in the open field. A proportion of Nrxn rats (5/16 rats) displayed a mounting behavior directed towards the male conspecific in the open field. None of the WT rats displayed this behavior (0/16 rats; Supplementary Figure 10a,b). This behavior was also observed to occur in pairs of Nrxn rats in their home cage, but was rarely observed in WT

pairs (eta^2=0.46, 95% C.I.=1.15 to 3.85, two-tailed unpaired t-test). The Nrxn rats also displayed normal exploration behavior in the elevated plus maze and open field (Supplementary Figure 9h,i), demonstrating that abnormally elevated anxiety is unlikely to underlie impaired social learning.

The physiological and behavioral data argue for a deficit of MeA function in Nrxn rats that leads to impairment of behaviors that rely on the LA-MeA path. Therefore, increased activation of the MeA may alleviate deficits of social fear conditioning in Nrxn rats. To test this, MeA was bilaterally chemogenetically activated in Wt and Nrxn rats (AAV-CaMKIIa-HA-rM3D(Gs)-IRES-mCitrine; DREADD-Gs[35], Supplementary Figure 11a–d) during social fear conditioning. Control Nrxn rats were transduced with a reporter only (AAV-CaMKIIa-EYFP). The effectiveness of DREADD-Gs at activating MeA neurons was assessed using in vivo extracellular recordings from anesthetized rats (as above). Administration of CNO caused an increase in the overall firing rate and number of spontaneously firing neurons recorded in the MeA of anesthetized DREADD-Gs rats, whereas vehicle had no significant effect (Supplementary Figure 11a–c; eta^2=0.38, two-way RM-ANOVA). The MeA was activated by CNO during social fear conditioning. Activation of MeA improved social fear conditioning in Nrxn rats, as demonstrated by increased freezing during conditioning (Figure 8a; eta^2=0.19, two-way RM-ANOVA) and in response to the socially conditioned context and CS+ cue when tested after 48 hours (Figure 8b; eta^2=0.64, one-way ANOVA; eta^2=0.12, two-way RM-ANOVA). This increased freezing was absent if the experiment was repeated with an anesthetized demonstrator (Figure 8c), indicating that MeA activation itself did not induce spurious freezing to tone or context (Figure 8c,d). Furthermore, DREADD-Gs activation of the MeA did not significantly increase conditioned freezing upon classical fear conditioning (Figure 8e), indicating that DREADD-Gs did not lead to abnormal elevation of fear behaviors that do not rely on MeA circuitry. This remarkable improvement in use of social information to guide behavior upon MeA activation was observed despite a lifetime with genetic abnormality and a history of MeA dysfunction.

Discussion

These results demonstrate that an intra-amygdala path between the LA and MeA underlies the ability to link the affective content of social cues with other external predictive cues. Specifically, the MeA was required to value a social cue emitted by a conspecific, while the LA-MeA circuit was required to assign value to environmental cues associated with social cues and subsequently use that environmental cue to guide behavior. The effects of LA-MeA pathway inactivation most readily support interpretation of the observations as impaired social learning instead of limited to impaired expression during learning. The reason for this is that if social fear learning was intact, but expression was transiently impaired due to DREADD inactivation, it is expected that expression of conditioned freezing would be observed when tested after 48 hours, but it was not. This is congruent with a role for the amygdala in processing social signals from faces and recognition of facial expression[1,5], and further adds the role of the LA-MeA in learning about and initiation of an affective response to the learned social cue. This places the LA-MeA as a specialized circuit that is parallel to BLA-CeA, BLA-BNST and BLA-NAc paths in the production of a coordinated response to

conditioned cues. The MeA is important for species-specific social behaviors; LA inputs to the MeA help select and guide the appropriate social behavior, and participate in broadening the importance of a social cue to associated environmental contingencies.

In addition to impairments in social learning caused by acute disruption of the LA-MeA path and the correlation between social learning and LA-MeA path strength, this specific amygdala circuit was abnormal in a condition of impaired social learning, the Nrxn knockout rat. Previous studies that utilized social interaction and social preferences behaviors of Nrxn knockout mice have found mixed results[30,31], consistent with the relatively subtle differences in social interaction observed here. Instead, a more robust social deficit of Nrxn rats appears in the processing of emotionally relevant social cues that signal environmental threats and assigning value to a cue with social importance. These impairments in Nrxn rats map closely to the impairments found upon disconnection between the LA and MeA, parallel the impaired function of this circuit, and share similarities with abnormalities observed after isolation rearing[36]. Activation of MeA by DREADD-Gs reduced these impairments, though this is not necessarily due to repair of the underlying pathophysiology. In addition, the observed pathophysiology in Nrxn knock-out rats may not reflect the etiology of social deficits in autism spectrum disorders, which are associated with loss-of-function heterozygous mutations instead of knock-out. Surprisingly few studies have tested the importance of the amygdala in genetic models associated with social abnormalities, such as those found in autism[37–42]. While informative, those few studies largely focused on the basolateral amygdala complex, and did not test the impact on intra-amygdala function. Furthermore, no previous studies have tested the importance of the LA-MeA intra-amygdala circuit in social behavior. The current study found very discrete, targetable, abnormalities in this circuitry associated with impaired social learning.

Use of DREADD-based manipulations causes prolonged but temporary changes in neuronal activity. However, it is not the same as a true inactivation, and the functional disconnection induced here is unlikely to be as complete as disconnections produced by pharmacological or anatomical approaches. In addition, while use of DREADDs here was demonstrated to cause a change in neuronal activity, it exerts effects by modulation of intracellular signaling, which may contribute to the observed outcomes upon DREADD-induced inactivation. DREADD expression was promoted by CaMKIIa or hSYn. While CaMK may be expressed in several BLA neuronal types, CaMKIIa expression is limited to BLA projection neurons[43], therefore use of the CaMKIIa promoter is expected to limit DREADD expression to projection neurons[20] as previously demonstrated[44], and use of this promoter with DREADD-Gi has been demonstrated to impact the physiology of BLA projection neurons[44,45]. In addition, expression was observed in fibers in regions that are LA projection targets, such as entorhinal cortex. While CaMKIIa expression can be observed in sections that include the posterior MeA[46,47], it is not entirely clear in which MeA neurons it is expressed. However, fibers were observed in hypothalamus and stria terminalis, indicating that DREADD expression included MeA projection neurons and these neurons may overlap with specific populations of MeA neurons that modulate social behavior[48].

Treatments for autism often rely on behavioral interventions that are less effective in severe autism. Our current results provide a rationale for pursuing approaches that augment MeA

function in combination with behavioral intervention. This may produce benefits in the development of social abilities despite social impairments from an early age.

Methods

All procedures were approved by the Rosalind Franklin University Institutional Animal Care and Use Committee, and complied with the Guide for the Care and Use of Laboratory Animals (National Research Council, 2011). Efforts were made to minimize animal suffering and to reduce the number of animals used.

Animal model

Male neurexin 1 knock-out (Nrxn) rats and wild type (WT) control rats (Sprague-Dawley background, Sage Labs/Horizon Discovery, Boyertown, PA) and standard Sprague-Dawley rats (Harlan, Indianapolis, IN) were obtained at 9–12 weeks old. The sex (male) and age (9–12 weeks) was the same across all experiments. The number of animals is indicated for each experiment. Nrxn knockout rats[27] were bred from homozygous pairs. Age-matched WT rats of the same genetic background were bred at the same facility, housed on the same rack/room and shipped at the same time. Rats were acclimated to the animal facility for at least 10 days before use. The rats were housed 2–3/cage in a climate-controlled facility with ad libitum access to food and water. Lights in the housing room were on a 12:12 hour reverse light-dark schedule. All rats were naïve at the initiation of experiments. All experiments were performed during the dark cycle.

Validation of Neurexin-1α knockout in rats—A subset of rats (4 neurexin KO and 5 WT controls) were deeply anesthetized with 5% isoflurane (Sigma-Aldrich, St. Louis, MO), decapitated, and brains were quickly extracted and flash frozen in bromobutane and methylbutane on dry ice and subsequently stored at −80°C until RNA or protein extraction.

For protein extraction, brains were homogenized in RIPA buffer with the addition of a proteinase inhibitor cocktail (Roche Diagnostic, Indianapolis, IN). Homogenates were centrifuged at 15,000 g for 20 minutes at 4°C then stored at −80°C. Protein (30μg) was separated by electrophoresis on an 8–16% Mini-PROTEAN® TGX™ gel (Bio-Rad Laboratories, Hercules, CA) for 15 minutes at 90 volts followed by 1.5 hours at 150 volts, then transferred to a nitrocellulose membrane for 1.5 hours at 110 volts. The membrane was blocked in 5% BSA and 0.1% Tween-20 in Tris- buffered saline (TBST) for 1 hour at room temperature, prior to overnight incubation with rabbit anti-Neurexin1α receptor antibody (1:1,000, catalog # ANR-031, Alomone Labs, Jerusalem, Israel; western blot validation on www.alomone.com and validation in Nrxn knock-out rats, Supplementary Figure 6) in 1% BSA/TBST at 4°C. Membranes were then washed with TBST (4 times for 10 minutes) and incubated with HRP-conjugated anti-rabbit secondary antibody (1:15,000; catalog #NA934VS, Amersham, GE Healthcare Bio-Sciences, Pittsburgh, PA; western blot validation on www.1degreebio.org and peer reviewed citations on www.bioz.com) for 1 hour at room temperature. The membrane was washed a final time with TBST (4 times for 10 minutes) then protein bands were developed with chemiluminescent detection reagent (ECL Select, Amersham) and exposed on autoradiographic film (Genesee Scientific, San Diego, CA). Blots were subsequently washed (4 times for 10 minutes) then re-probed with chicken

anti-α-tubulin (1:10,000, Sigma-Aldrich, catalog #SAB3500023; western blot validation on www.sigma-aldrich.com and peer reviewed citations on www.bioz.com) for 1 hour at room temperature, followed by a series of washes (4 times 10 minutes), incubation of HRP-conjugated goat anti – chicken secondary antibody (1:20,000; catalog #ab97135, Abcam, Cambridge, MA; western blot validation on www.abcam.com and peer reviewed citations on www.bioz.com), and a final set of washes (4 times 10 minutes) before being developed with chemiluminescent detection reagent (Amersham ECL Select) and exposed on autoradiographic film. Individual band densities were obtained with Image J software (NIH), and normalized to corresponding α-tubulin band densities.

Brain tissues were also separately processed for RNA extraction with Trizol Reagent (Life Technologies, Thermo Fisher Scientific, Waltham, MA) according to manufacturers' protocol. Total RNA was treated with DNAse I enzyme (Thermo Fisher Scientific) and reverse transcribed using recombinant M-MuLV reverse transcriptase (Thermo Fisher Scientific) into cDNA template. Jumpstart™ Taq Readymix™ (Sigma) was used to amplify cDNA utilizing the following primers: GAPDH forward (5′ – GACATGCCGCCTGGAGAA – 3′), GAPDH reverse (5′ – AGCCCAGGATGCCCTTTAGT – 3′), Neurexin-1α forward (5′ – ATGTAGAAGGTCTGGCGCAC – 3′), and Neurexin-1α reverse (5′ – ATTTCGTCGCTGCTGCTTTG – 3′). PCR cycling conditions for both GAPDH and Neurexin-1α were as follows: 94°C for 2 minutes, 30 cycles of 95°C for 30 seconds, 60°C for 30 seconds, 72°C for 1 minute, followed by 5 minutes at 72°C. PCR products were separated on a 2.5% agarose gel, visualized with ultraviolet light (FOTO/UV® 26) and images were acquired (12-megapixel resolution, iPhone 6S, Apple Inc, Cupertino, CA) from 12 inches above the gel, without flash). Band densities were obtained from these images by Image J Software (NIH) and normalized to GAPDH cDNA.

Chemogenetic surgical procedure

To induce DREADD expression in the MeA or LA, adeno-associated viral (AAV5) vectors with plasmid for DREAAD receptors (Dr. Bryan Roth, UNC Vector Core, Chapel Hill, NC) were injected intracranially. Rats were randomly assigned to the different groups. Rats were anesthetized with either an intraperitoneal (i.p.) cocktail of ketamine (80–100 mg/kg; Webster Veterinary Supply, Devens, MA) and xylazine (10–20 mg/kg; Webster Veterinary Supply) or isoflurane (5% induction, 2–3% maintenance; Sigma-Aldrich). After confirmation of anesthesia, meloxicam (Metacam, 1 mg/kg, s.c.) was injected, rats were placed in blunt ear bars of a stereotaxic apparatus (David Kopf Instruments, Tujunga, CA), and their scalp was shaved and wiped with betadine and ethanol (70%). A small incision was made and 1% procaine was placed on the skull. Burr holes were drilled over the LA (A-P −3.3 mm, M-L 5.0 mm, D-V −8.0 mm), MeA (A-P −3.0 mm, M-L 3.3 mm, D-V −9.0 mm), or both, based on the atlas of Paxinos and Watson[49]. DREADD-Gi (AAV-CaMKIIa-HA-hM4D(Gi)-IRES-mCitrine), DREADD-Gs (AAV-CaMKIIa-HA-rM3D(Gs)-IRES-mCitrine), AAV-CaMKIIa-EYFP, or both Cre-dependent DREADD-Gi (AAV-hSyn-DIO-hM4D(Gi)-mCherry) and CAV2-Cre (Plateforme de Vectorologie de Montpellier, Institut de Génétique Moléculaire de Montpellier) was infused (0.5 μL/locus) through a small bore stainless steel cannula (33 g), driven by an infusion pump at 50–100 nL/min (PHD 2000 infusion pump,

Harvard Apparatus, Holliston, MA). The cannula remained in place for 5 minutes before withdrawal. The incision was cleaned and stapled, and the rat was returned to its home cage after full mobility was regained. For 48 hours after surgery, rats were administered a daily analgesic (1 mg/kg meloxicam, s.c.). Behavior procedures began after 2–3 weeks.

Immunohistochemical validation of infusion sites—At the conclusion of experiments that used rAAV-HA-DREAD, immunostaining was performed for the HA tag of the plasmid. Brains were fixed in 4% paraformaldehyde at 4 degrees C for 12–24 hours then transferred to 30% sucrose in phosphate-buffered saline (PBS) for at least 2 days. Brains were sectioned (50 μm), permeabilized (0.4% Triton in PBS for 1 hour at room temperature), and blocked (1% bovine serum albumin/5% normal goat serum in 0.4% Triton/PBS). Sections were incubated with the primary antibody (HA-tag Rabbit monoclonal antibody, 1:500; Cell Signaling Technology, catalog #3724; western blot validation on www.cellsignal.com and peer reviewed citations for immunohistochemistry on www.bioz.org) overnight at 4°C, washed (0.4% Triton/PBS, 10 min, 3 times), then incubated with secondary antibody (Alexa Fluor 488 goat anti-rabbit, 1:250; Invitrogen, Thermo-Fisher Scientific catalog #A-11008; immunohistochemistry validation on www.thermofisher.com and peer reviewed citations for immunohistochemistry on www.bioz.org[50]) for 2 hours at room temperature. Sections were then washed (as above), and mounted on slides. Fluorescence was viewed and plotted to determine the location of DREADD expression.

At the conclusion of experiments that used rAAV-DIO-DREAD with CAV-Cre, immunostaining was performed for Cre-recombinase and mCherry to verify infusion sites. Free-floating brain sections (50 μm) were washed 3 times for 10 minutes in 0.1M PBS (pH = 7.4), then incubated in 0.4% Triton X-100/0.1M PBS for 1 hour at RT. Tissue was then blocked in 1% BSA/5% NGS/0.4% Triton X-100/0.1M PBS for 3 hours at room temperature followed by an overnight incubation in rabbit anti-Cre Recombinase (1:750, Biolegend, catalog #908001[51]) with 0.4% Triton X-100/0.1M PBS at 4°C. The following day, sections were washed (6 times for 10 minutes) and incubated in Alexa Fluor® 488 goat anti-rabbit (1:750, Life Technologies, catalog #A11008, validation as descibed for Alexa Fluor 488 above) for 2 hours at RT. Tissue was washed again (6 times for 10 minutes) then sections were mounted and coverslips were applied with Fluromount mounting media (Sigma). Sections were imaged (Nikon E600 microscope, Melville, NY) and Cre-Recombinase and mCherry expression were mapped to identify location of neurons transduced with CAV2-Cre-Recombinase and AAV8-hSyn-DIO-hM4D(Gi)-mCherry respectively. Only animals with successful viral transduction were included in data analysis. Images were acquired (Olympus Fluoview 10 Scanning Laser confocal microscope or Nikon E600 microscope) and post-acquisitional analysis was performed using Fluoview software (Olympus America, Center Valley, PA) and Adobe Photoshop (Adobe Systems, San Jose, CA).

Behavior

All behavioral activity was filmed with IR-sensitive cameras (Fire-i, Unibrain, San Ramon, CA), fed to a computer (Dell E6500, Round Rock, TX), and saved for offline analysis using AnyMaze software (Wood Dale, IL). Where indicated, rats were injected with saline vehicle

or clozapine-N-oxide (CNO, 1 mg/kg, i.p.) 40 minutes before the behavioral test. The number of animals used for behavioral experiments was determined by sample size calculations based on the expected effect size in a previous study[18]. For all experiments that utilized DREADDs or Nrxn rats, the experimenter performing the behavioral study was blind to the treatment groups or genotype of the rat. Rats were randomly assigned to groups. When animals underwent multiple behavioral tests, they occurred in this order: open field, social interaction test, novel object exploration test, novel object-novel rat exploration. Rats were excluded from the study if there was a failure of equipment.

Open field—Open field exploration was conducted in a dimly lit room (20–25 lux) with computer-generated white noise (65–70 dB). A rat was placed individually into the open field (black opaque, 24×35 in) for 5 min. Total distance, speed, and time in the center and periphery of the field were quantified.

Social interaction—After open field exploration, a novel rat was added to the field for 5 min. The novel rat was WT Sprague-Dawley within 50 g body weight of the subject rat. The novel rats all had a minimum of 10 min prior exposure to the open field. The number and time of social interaction was quantified. The type of social interaction was noted (aggressive or exploratory). Rats with DREADD expression underwent the social interaction test two times (48 hours apart), once with vehicle and once with CNO in a counterbalanced manner. In a separate experiment, cohabitating WT pairs and Nrxn pairs were observed in their home cages in the housing room (15 min observation, each pair observed 4 times). The number of aggressive episodes (mounting) and the number of play episodes were quantified.

Novel object exploration—1–3 days after social interaction was performed, the rat was returned to the open field (same conditions as above). During this test the open field contained a novel object. Novel object exploration was defined as physical manipulation of the object or sniffing of the object. The number and time of exploration of the novel object was quantified.

Novel object - Novel rat exploration—During this test, subject rats were placed in the open field (conditions as above) that contained a novel object suspended from a string (2–3 cm above floor of open field) and a novel rat. The novel rat was WT Sprague-Dawley within 50 g body weight of the subject rat, and had a minimum of 10 min prior exposure to the open field. The number and time of exploration of the novel object and the novel rat was quantified.

Odor exploration—To verify that the WT and Nrxn rats have sufficient olfactory ability, the following tests were performed.

(i) Sucrose pellet detection: Rats were given grape-flavored sucrose pellets in their home cage one day prior to testing to produce familiarity before the test. During the test, rats were placed in a novel polycarbonate container ($17 \times 8.5 \times 8$ height, in inches) with fresh bedding. Under the bedding were 6 grape-flavored sucrose pellets. The latency to find the first pellet was measured.

(ii) Female odor approach: During this test, subject rats were placed in the open field (conditions as above), with a glass dish (10 cm diameter, 2 cm height) of bedding in opposite corners. One dish of bedding was from a cage of novel cycling adult female rats, the other dish of bedding was from a cage of novel male adult rats. The number and time of exploration of each tray was quantified.

Standard cued fear conditioning—Cued fear conditioning and testing were performed in different chambers with distinct contexts (wall pattern and color, odors, and flooring) as described previously[18]. Rats were placed in a chamber (10.6″ 25x 10.625″ × 14.125″ height or 13.5″ × 10″ × 12″ height, counterbalanced across groups) with stainless steel grid floor. The chamber was housed inside a sound attenuating cabinet (UGO Basile, VA, Italy; 21″ in. X 17.5″ in. X 21.25″ in. height) with dim light (~20 lux) with an additional infrared LED light, and constant white noise (70 dB) produced by a fan. A ceiling mounted digital camera that was sensitive to light in the IR range was used to record behavior. Chambers were cleaned with ethanol (50%) prior to behavioral procedures and between each subject. Rats were allowed to explore the chamber freely. After a 180 s habituation period, a tone (2 kHz, 85 dB, 10 s duration) was presented. At the last second of the tone, a foot shock was presented (1 s duration, 0.4 – 0.5 mA intensity depending on chamber), such that the shock and the tone co-terminated. This was repeated 4 times at 60 s inter-trial intervals. Rats remained in the chamber for 1 min after the end of the last conditioning trial, and were then returned to their home cage. After 48 hours, conditioned freezing was tested in the same context and cued conditioned freezing and within session extinction were tested in a novel context. The contextual freezing test lasted 5 minutes. The cued conditioned freezing consisted of a 3 min habituation followed by 15 trials of tone presentation (20s, 85 dB) at a 60s inter-trial interval. No foot shock was presented during testing trials. Freezing was quantified by AnyMaze software based on a threshold of change in video image pixels. A freezing episode had to last a minimum of 1 s to be included in the software analysis. These criteria were compared against visually confirmed freezing (behavioral immobility except for movement associated with respiration). Total freezing during each trial (entire 60s) was used as an index of conditioned fear and converted to a percentage ([time of freezing/60s] × 100) for analysis. Data from one animal were excluded due to mechanical failure.

Foot shock intensity was determined from a separate group of rats. Foot shock was delivered through the floor grid in 0.1 mA increments from 0.2 mA (0.2 mA, 0.3 mA, 0.4 mA, 0.5 mA) until a forepaw withdrawal with an avoidance response (e.g. backpedaling) was noted. Based on analysis of this response, a foot shock intensity of 0.4 mA was found to be appropriate for one conditioning chamber, and 0.5 mA was found to be appropriate for the other. There was no significant difference between groups in this threshold response to foot shock for each chamber (see Results). Conditioning chambers were counterbalanced across groups.

Social cued fear conditioning—Social fear conditioning was performed similarly to a previous study[18]. The conditioning chamber (as above) was separated in half with a vinyl coated wire mesh divider (3/4 inch mesh) in a plexiglass frame. The floor of one half was a stainless steel grid, the other half was a plexiglass panel. The demonstrator rat was placed

into the side with exposed stainless steel grid. The demonstrator rat was always a WT rat. The observer rat was placed into the side with the plexiglass floor. Upon placement in the chamber, rats were given 180 s to habituate. Following habituation, a tone (10 s, 2 kHz, 85 dB) was presented to the chamber. At the end of the tone, foot shock (0.5 – 0.6 mA, 1 s, co-terminating with tone) was delivered through the stainless steel floor grid to the demonstrator rat. The observer rat was fully isolated from foot shock. This was repeated 6 times, at an interval of 60 s. After 48 hours, contextual freezing was measured from individual rats by placing the rat into the same chamber that was used for conditioning for 5 min. The rat was then placed into a novel chamber (contextually distinct in wall pattern, size, shape, and odor) for 120 s habituation followed by tone presentation (20 s, 2 kHz, 85 dB). The tone was repeated 12 times at an interval of 60 s. Freezing during each trial was measured (as above), along with nose poking through the mesh divider, location of the observer rat, and social interaction during conditioning. Social cued conditioning was performed once per rat, unless noted. In those instances, the second conditioning was performed in a context that was distinct from the original context.

Electrophysiology

The number of rats and neurons for electrophysiological experiments was determined by sample size calculations with an expected effect size estimated from preliminary data.

In vivo electrophysiology—Rats were anesthetized with urethane (1.5 g/kg, i.p.; Sigma-Aldrich Corp.) and their ears were infiltrated with 2% lidocaine hydrochloride jelly. Upon verification of anesthesia, rats were placed into a stereotaxic apparatus (David Kopf Instruments or Stoelting Instruments, Wood Dale, IL). Core body temperature was monitored rectally and maintained near 37° C with a heating pad (TC-1000 Temperature Controller, CWE Inc, Ardmore, PA). An incision was made on the scalp and bore holes were drilled over the LA (A-P −3.3 mm, M-L 5.0 mm, D-V −8.0 mm) and posterior MeA (A-P −3.0 mm, M-L 3.3 mm, D-V −9.0 mm). A concentric bipolar stimulation electrode (0.25 mm outer diameter; Rhodes Medical Instrument) was lowered into LA or MeA. This electrode was used to record intra-amygdala spontaneous field potentials to gauge anesthesia state and to deliver electric stimulation. A glass microelectrode (2.0 mm outer diameter borosilicate glass) was heat-pulled (PE-2 microelectrode puller, Narishige Group, Tokyo, Japan) and filled with 2% Pontamine Sky Blue (Alfa Aesar, Ward Hill, MA) in 2 M NaCl (Thermo Fisher Scientific), with an in situ resistance of 10–20 MOhms. The glass electrode was lowered slowly to the amygdala via hydraulic microdrive (Model MO-10, Narishige Group). Signals were filtered and amplified (2400 Extracellular Preamplifier, Dagan Corp., Minneapolis, MN or Model 1800 amplifier, A-M Systems, Carlsborg, WA), and monitored audially (AM10 amplifier, Grass Technologies, Warwick, RI). Signals were digitized (5–10 kHz; InstruTECH ITC-18, HEKA Instruments, Bellmore, NY) and fed to a computer (Mac Pro, Apple Inc), visualized online (AxoGraph X, Australia) and saved for later analysis. Electrical stimulation was delivered (S88 Stimulator and PSIU6 Stimulation Isolation Unit, Grass Technologies) through the bipolar electrode with an intensity range of 0.1 to 0.9 mA, 0.2 ms duration, repeating at 0.2 Hz. Responses that displayed polysynaptic or antidromic characteristics were not included in analysis. To minimize spread of stimulation current between LA and MeA and reduce risk of measurement of a non-specific response, three

approaches were used: 1) stimulation intensity was kept below 1.0 mA, 2) the distance between stimulation electrodes was consistently >2.0 mm apart, and 3) the latency of monosynaptic responses had to be greater than 3.0 ms. The stimulation site had to be histologically confirmed to lie within the LA. Further confirmation that current spread is not likely to underlie the obtained results can be obtained from the finding that stimulation sites that were mispositioned medially (i.e. closer to MeA and in the central amygdala) did not evoke monosynaptic excitatory responses (0/18 neurons from 4 animals).

At the conclusion of experiments, Pontamine was iontophoresed (−30 μA) from the recording electrode using constant current for 30–45 min. The rat was euthanized and the brain was placed in 4% formaldehyde (Electron Microscopy Sciences) in 0.1 M phosphate buffer overnight, and then cryoprotected in 30% sucrose (Sigma-Aldrich) in 0.1 M phosphate buffer. Brains were sectioned (60 μm thick) with a freezing microtome (Leica Microsystems Inc, Buffalo Grove, IL) and stained with cresyl violet (Sigma Aldrich Corp.). Recording and stimulation sites were verified by light microscopy. Data were excluded if recording or stimulation sites were outside the borders of the MeA or LA.

In vitro electrophysiology—Rats were anesthetized with a cocktail of ketamine (80–100 mg/kg; Webster Veterinary Supply) and xylazine (10–20 mg/kg; Webster Veterinary Supply). Upon confirmation of anesthesia, rats were intracardially perfused with ice cold, aerated (95% O_2/5% CO_2) high sucrose artificial cerebrospinal fluid (ACSF) containing (in mM) 2.5 KCl, 1.25 NaH_2PO_4, 25 $NaHCO_3$, 7 dextrose, 7 $MgCl_2$, 0.5 $CaCl_2$, 210 sucrose, 1.3 ascorbic acid, 3 sodium pyruvate. Osmolality of high sucrose ACSF was approximately 290 mOsm. The rate of perfusion was approximately 4 mL/min with a total volume of 20–30 mL. Rats were decapitated and the brain was removed quickly. The brain was sectioned coronally at 300 μm in a vibratome (Ted Pella, Inc., Redding, CA) in ice-cold high sucrose ACSF, and brain slices were placed for approximately 1 h at 34°C in physiological ACSF containing (in mM) 125 NaCl, 2.5 KCl, 1.25 NaH_2PO_4, 25 $NaHCO_3$, 10 dextrose, 1 $MgCl_2$ and 2 $CaCl_2$, with the addition of 1.3 mM ascorbic acid and 3 mM sodium pyruvate. Recordings were performed at 32–34°C in submerged slices in physiological ACSF (as above, without ascorbic acid or sodium pyruvate). (+)-bicuculline (10 μM; Ascent Scientific, Princeton, NJ; dissolved in dimethyl sulfoxide), picrotoxin (10 μM; dissolved in ethanol), 6-cyano-7-nitroquinoxaline-2,3-dion (CNQX) disodium salt (10 μM; Ascent Scientific, Princeton, NJ; dissolved in ddH_2O) and DL-2-Amino-5-phosphonopentanoic acid (DL-AP5) sodium salt (50 μM; abcam Biochemicals, Cambridge, MA; dissolved in 100mM NaOH) were added to the ACSF as noted to block GABAA-, AMPA- and NMDA receptor mediated currents. Final solvent concentrations were <0.1% of the total ACSF volume. Solutions were continuously aerated with 95% O_2/5% CO_2.

Electrodes (1.8 – 11.5 MΩ open tip resistance) for recording of voltage were filled with an intracellular solution containing (in mM) 120 K-gluconate, 20 KCl 0.2 EGTA, 10 HEPES, 2 NaCl, 4 ATP-Mg, 0.3 GTP-Tris, 7 Tris-phosphocreatine, and 0.2% neurobiotin (Vector Laboratories, Inc., Burlingame, CA), with a pH of 7.3. Electrodes for recording of currents were filled with an intracellular solution containing (in mM) 150 CsCl, 0.2 EGTA, 10 HEPES, 2 NaCl, 4 ATP-Mg, 0.3 GTP-Tris, 7 Tris-phosphocreatine, 5 QX314 chloride (Ascent Scientific, Princeton, NJ) and 0.2% neurobiotin (Vector Laboratories, Inc.). Whole-

cell recordings were performed in voltage clamp or bridge mode from visually identified neurons within LA or posterior MeA (AxoClamp 2B, Molecular Devices, Inc., Sunnyvale, CA). Signals were low-pass filtered at 3–5 kHz and digitalized at 10–20 kHz (InstruTECH ITC-18, HEKA Instruments). Mean series resistance for each group was below 25 MΩ. All electrophysiology data were monitored with AxoGraph X software and stored on a computer (Mac Pro, Apple Inc) for off-line analysis.

After recordings, slices were fixed in 4% paraformaldehyde in 0.1 M phosphate-buffered saline (PBS) for up to four weeks at 4°C. Sections were rinsed three times with PBS, treated with Triton X-100 (VWR international, Radnor, PA; 1% in PBS) for 6 to 8 hours and then incubated in the Vectastain ABC Reagent (Vector Laboratories) in PBS at room temperature overnight. After three rinses with PBS, sections were reacted with diaminobenzidine (DAB) and H_2O_2 (Peroxidase Substrate Kit DAB, Vector Laboratories) in water to visualize the neurobiotin-filled neurons. Sections were washed in PBS repeatedly to stop the reaction. Sections were mounted, dried and coverslipped. Stained sections were used to confirm principle neuron morphology and localize the recording sites.

Statistical analysis

Data analysis was performed using GraphPad Prism software (La Jolla, CA). Significance was set at $p < 0.05$. Data were tested for normal distribution (Kolmgorov-Smirnov test) and homogeneity of variance (Bartlett's test). All data that were compared with parametric statistical tests met these assumptions. Planned comparisons between two groups were performed with two-tailed unpaired t-test, and between three groups with one-way ANOVA (e.g. Time proximal to divider, Time nose poking divider, Contextual freezing, Firing rate, Number of neurons/track, Input resistance, mEPSC frequency, paired-pulse ration, CV of EPSC, Auditory-induced freezing, Latency to find sucrose pellets, Shock threshold, Time in open arms of elevated plus maze). Comparisons between two or more groups on multiple factors were performed with two-way ANOVA or two-way repeated measures (RM)-ANOVA, if repeated measures from the same subject were obtained (e.g. Fear conditioning freezing, Cued freezing, Social interaction (vehicle and CNO), Slope of field potential, Excitability, Time in open field center (high vs low lux), Novel bedding exploration (male vs female)). Significance in the ANOVA test was followed by Holm-Sidak's multiple comparisons test to compare groups. Significant effect sizes (eta^2 and confidence interval (C.I. where appropriate) are included in text, with full comparison details in figure legends. Data are presented as group mean ± 95% confidence interval, unless otherwise indicated.

Supplementary Material

Refer to Web version on PubMed Central for supplementary material.

Acknowledgments

References

1. Adolphs R, Tranel D, Damasio H, Damasio A. Impaired recognition of emotion in facial expressions following bilateral damage to the human amygdala. Nature. 1994; 372:669–672. [PubMed: 7990957]

2. Brothers L, Ring B, Kling A. Response of neurons in the macaque amygdala to complex social stimuli. Behav Brain Res. 1990; 41:199–213. [PubMed: 2288672]

3. Dicks D, Myers RE, Kling A. Uncus and amiygdala lesions: effects on social behavior in the free-ranging rhesus monkey. Science. 1969; 165:69–71. [PubMed: 17840690]

4. Ferguson JN, Aldag JM, Insel TR, Young LJ. Oxytocin in the medial amygdala is essential for social recognition in the mouse. J Neurosci. 2001; 21:8278–8285. [PubMed: 11588199]

5. Morris JS, et al. A differential neural response in the human amygdala to fearful and happy facial expressions. Nature. 1996; 383:812–815. [PubMed: 8893004]

6. Meyer-Lindenberg A, et al. Neural correlates of genetically abnormal social cognition in Williams syndrome. Nat Neurosci. 2005; 8:991–993. [PubMed: 16007084]

7. Stanfield AC, et al. Towards a neuroanatomy of autism: a systematic review and meta-analysis of structural magnetic resonance imaging studies. Eur Psychiatry. 2008; 23:289–299. [PubMed: 17765485]

8. Amorapanth P, LeDoux JE, Nader K. Different lateral amygdala outputs mediate reactions and actions elicited by a fear-arousing stimulus. Nat Neurosci. 2000; 3:74–79. [PubMed: 10607398]

9. Goosens KA, Maren S. Contextual and auditory fear conditioning are mediated by the lateral, basal, and central amygdaloid nuclei in rats. Learn Mem. 2001; 8:148–155. [PubMed: 11390634]

10. Namburi P, et al. A circuit mechanism for differentiating positive and negative associations. Nature. 2015; 520:675–678. [PubMed: 25925480]

11. Pitkanen A, et al. Intrinsic connections of the rat amygdaloid complex: projections originating in the lateral nucleus. J Comp Neurol. 1995; 356:288–310. [PubMed: 7629320]

12. Hong W, Kim DW, Anderson DJ. Antagonistic control of social versus repetitive self-grooming behaviors by separable amygdala neuronal subsets. Cell. 2014; 158:1348–1361. [PubMed: 25215491]

13. Maras PM, Petrulis A. Chemosensory and steroid-responsive regions of the medial amygdala regulate distinct aspects of opposite-sex odor preference in male Syrian hamsters. Eur J Neurosci. 2006; 24:3541–3552. [PubMed: 17229102]

14. Meredith M, Westberry JM. Distinctive responses in the medial amygdala to same-species and different-species pheromones. J Neurosci. 2004; 24:5719–5725. [PubMed: 15215294]

15. Unger EK, et al. Medial amygdalar aromatase neurons regulate aggression in both sexes. Cell Rep. 2015; 10:453–462. [PubMed: 25620703]

16. Knapska E, et al. Between-subject transfer of emotional information evokes specific pattern of amygdala activation. Proc Natl Acad Sci U S A. 2006; 103:3858–3862. [PubMed: 16497832]

17. Cook M, Mineka S. Selective associations in the observational conditioning of fear in rhesus monkeys. J Exp Psychol Anim Behav Process. 1990; 16:372–389. [PubMed: 2230660]

18. Yusufishaq S, Rosenkranz JA. Post-weaning social isolation impairs observational fear conditioning. Behav Brain Res. 2013; 242:142–149. [PubMed: 23295398]

19. Armbruster BN, Li X, Pausch MH, Herlitze S, Roth BL. Evolving the lock to fit the key to create a family of G protein-coupled receptors potently activated by an inert ligand. Proc Natl Acad Sci U S A. 2007; 104:5163–5168. [PubMed: 17360345]

20. Zhu H, et al. Chemogenetic inactivation of ventral hippocampal glutamatergic neurons disrupts consolidation of contextual fear memory. Neuropsychopharmacology. 2014; 39:1880–1892. [PubMed: 24525710]

21. Nader K, Majidishad P, Amorapanth P, LeDoux JE. Damage to the lateral and central, but not other, amygdaloid nuclei prevents the acquisition of auditory fear conditioning. Learn Mem. 2001; 8:156–163. [PubMed: 11390635]

22. Ecker C, et al. Brain anatomy and its relationship to behavior in adults with autism spectrum disorder: a multicenter magnetic resonance imaging study. Arch Gen Psychiatry. 2012; 69:195–209. [PubMed: 22310506]

23. Richey JA, et al. Common and distinct neural features of social and non-social reward processing in autism and social anxiety disorder. Soc Cogn Affect Neurosci. 2014; 9:367–377. [PubMed: 23223206]

24. Jamain S, et al. Mutations of the X-linked genes encoding neuroligins NLGN3 and NLGN4 are associated with autism. Nat Genet. 2003; 34:27–29. [PubMed: 12669065]

25. Kim HG, et al. Disruption of neurexin 1 associated with autism spectrum disorder. Am J Hum Genet. 2008; 82:199–207. [PubMed: 18179900]

26. Missler M, et al. Alpha-neurexins couple Ca2+ channels to synaptic vesicle exocytosis. Nature. 2003; 423:939–948. [PubMed: 12827191]

27. Esclassan F, Francois J, Phillips KG, Loomis S, Gilmour G. Phenotypic characterization of nonsocial behavioral impairment in neurexin 1alpha knockout rats. Behav Neurosci. 2015; 129:74–85. [PubMed: 25420124]

28. Maximov A, Sudhof TC. Autonomous function of synaptotagmin 1 in triggering synchronous release independent of asynchronous release. Neuron. 2005; 48:547–554. [PubMed: 16301172]

29. Schoch S, et al. SNARE function analyzed in synaptobrevin/VAMP knockout mice. Science. 2001; 294:1117–1122. [PubMed: 11691998]

30. Etherton MR, Blaiss CA, Powell CM, Sudhof TC. Mouse neurexin-1alpha deletion causes correlated electrophysiological and behavioral changes consistent with cognitive impairments. Proc Natl Acad Sci U S A. 2009; 106:17998–18003. [PubMed: 19822762]

31. Grayton HM, Missler M, Collier DA, Fernandes C. Altered social behaviours in neurexin 1alpha knockout mice resemble core symptoms in neurodevelopmental disorders. PLoS One. 2013; 8:e67114. [PubMed: 23840597]

32. Debiec J, Sullivan RM. Intergenerational transmission of emotional trauma through amygdala-dependent mother-to-infant transfer of specific fear. Proc Natl Acad Sci U S A. 2014; 111:12222–12227. [PubMed: 25071168]

33. Kim EJ, Kim ES, Covey E, Kim JJ. Social transmission of fear in rats: the role of 22-kHz ultrasonic distress vocalization. PLoS One. 2010; 5:e15077. [PubMed: 21152023]

34. Takahashi Y, et al. Olfactory signals mediate social buffering of conditioned fear responses in male rats. Behav Brain Res. 2013; 240:46–51. [PubMed: 23183219]

35. Guettier JM, et al. A chemical-genetic approach to study G protein regulation of beta cell function in vivo. Proc Natl Acad Sci U S A. 2009; 106:19197–19202. [PubMed: 19858481]

36. Adams T, Rosenkranz JA. Social Isolation During Postweaning Development Causes Hypoactivity of Neurons in the Medial Nucleus of the Male Rat Amygdala. Neuropsychopharmacology. 2016; 41:1929–1940. [PubMed: 26677945]

37. Adachi M, Autry AE, Covington HEr, Monteggia LM. MeCP2-mediated transcription repression in the basolateral amygdala may underlie heightened anxiety in a mouse model of Rett syndrome. J Neurosci. 2009; 29:4218–4227. [PubMed: 19339616]

38. Babaev O, et al. Neuroligin 2 deletion alters inhibitory synapse function and anxiety-associated neuronal activation in the amygdala. Neuropharmacology. 2015

39. Jung SY, et al. Input-specific synaptic plasticity in the amygdala is regulated by neuroligin-1 via postsynaptic NMDA receptors. Proc Natl Acad Sci U S A. 2010; 107:4710–4715. [PubMed: 20176955]

40. Kim J, et al. Neuroligin-1 is required for normal expression of LTP and associative fear memory in the amygdala of adult animals. Proc Natl Acad Sci U S A. 2008; 105:9087–9092. [PubMed: 18579781]

41. Lee EJ, et al. Trans-synaptic zinc mobilization improves social interaction in two mouse models of autism through NMDAR activation. Nat Commun. 2015; 6:7168. [PubMed: 25981743]

42. Suvrathan A, Hoeffer CA, Wong H, Klann E, Chattarji S. Characterization and reversal of synaptic defects in the amygdala in a mouse model of fragile X syndrome. Proc Natl Acad Sci U S A. 2010; 107:11591–11596. [PubMed: 20534533]

43. McDonald AJ, Muller JF, Mascagni F. GABAergic innervation of alpha type II calcium/calmodulin-dependent protein kinase immunoreactive pyramidal neurons in the rat basolateral amygdala. J Comp Neurol. 2002; 446:199–218. [PubMed: 11932937]

44. Rei D, et al. Basolateral amygdala bidirectionally modulates stress-induced hippocampal learning and memory deficits through a p25/Cdk5-dependent pathway. Proc Natl Acad Sci U S A. 2015; 112:7291–7296. [PubMed: 25995364]

45. Li C, Rainnie DG. Bidirectional regulation of synaptic plasticity in the basolateral amygdala induced by the D1-like family of dopamine receptors and group II metabotropic glutamate receptors. J Physiol. 2014; 592:4329–4351. [PubMed: 25107924]

46. Chang BH, Mukherji S, Soderling TR. Calcium/calmodulin-dependent protein kinase II inhibitor protein: localization of isoforms in rat brain. Neuroscience. 2001; 102:767–777. [PubMed: 11182241]

47. Erondu NE, Kennedy MB. Regional distribution of type II Ca2+/calmodulin-dependent protein kinase in rat brain. J Neurosci. 1985; 5:3270–3277. [PubMed: 4078628]

48. Choi GB, et al. Lhx6 delineates a pathway mediating innate reproductive behaviors from the amygdala to the hypothalamus. Neuron. 2005; 46:647–660. [PubMed: 15944132]

49. Paxinos, CWG. By George Paxinos - The Rat Brain in Stereotaxic Coordinates. 6. Elsevier Science; 2009.

50. Bian X, Yanagawa Y, Chen WR, Luo M. Cortical-like functional organization of the pheromone-processing circuits in the medial amygdala. J Neurophysiol. 2008; 99:77–86. [PubMed: 17977926]

51. Keshavarzi S, Sullivan RK, Ianno DJ, Sah P. Functional properties and projections of neurons in the medial amygdala. J Neurosci. 2014; 34:8699–8715. [PubMed: 24966371]
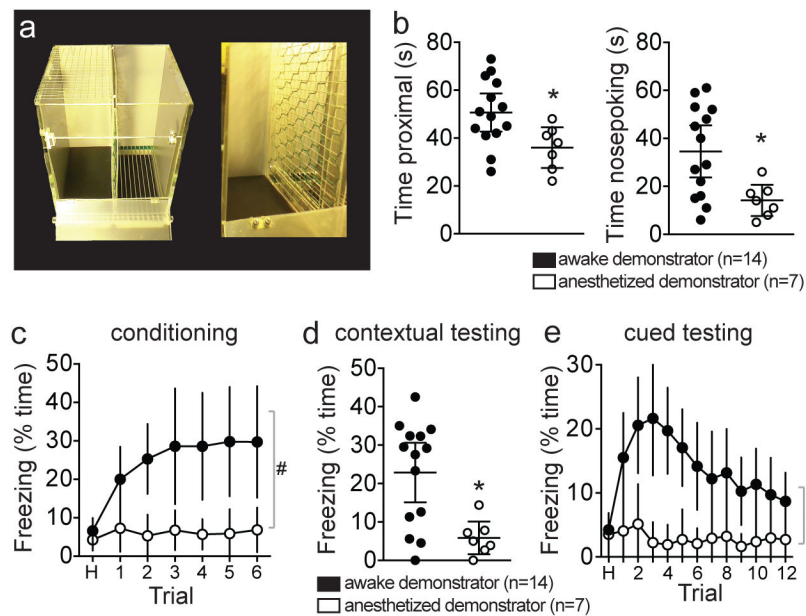
Figure 1. Fear learning through social transmission

a) The social fear conditioning apparatus (left) was divided down the middle to allow foot shock delivery paired with a tone to the animal on the right side (demonstrator), while the animal on the left received no foot shock (observer). The animals were separated by a mesh divider (right). **b**) Observer rats (n=14 rats) displayed exploratory behavior directed towards the demonstrator, measured as amount of time spent proximal to the divider that separated the rats (left) and amount of time spent with its nose in close proximity or poking into the divider (right). If the rat on the other side of the divider was anesthetized, the observer rat (n=7 rats) displayed significantly less time engaged in this social exploratory behavior (time proximal, p=0.0206, t=2.524, df=19, eta^2=0.25, 95% C.I.=−26.8 to −2.5, two-tailed unpaired t-test; time nose poking, p=0.0128, t=2.749, df=19, eta^2=0.29, 95% C.I.=−35.9 to −4.9, two-tailed unpaired t-test). **c**) Observer rats (n=14 rats) displayed increased freezing over the course of social fear learning (6 trials; p=0.0108, $F_{(6,91)}$=5.423, eta^2=0.29, one-way RM-ANOVA) if the demonstrator rat was awake, despite no physical contact with shock. However, if the demonstrator rat was anesthetized during the social fear conditioning, the observer rats (n=7 rats) displayed no significant freezing (p=0.5875, $F_{(6,42)}$=0.6337, eta^2=0.10, one-way RM-ANOVA), resulting in a significant difference in freezing between groups (i.e. difference in the effect of social fear conditioning; trial x anesthesia interaction, p=0.0446, $F_{(6,114)}$=2.237, eta^2=0.031, two-way RM-ANOVA; main effect of anesthesia p=0.0108, $F_{(1,19)}$=7.988, eta^2=0.19, two-way RM-ANOVA). **d**) When replaced in the same chamber after 48 hours, rats that were paired with an awake demonstrator (n=14 rats) displayed contextual freezing, while rats that were paired with an anesthetized demonstrator (n=7 rats) displayed significantly less contextual freezing (p=0.0045, t=3.219, df=19, eta^2=0.35, 95% C.I.=5.9 to 28.0, two-tailed unpaired t-test). **e**) Similarly, when placed in a novel chamber, and presented with the conditioned tone (CS+; 12 trials), rats that were paired with an awake demonstrator displayed conditioned freezing to the CS+ (n=14 rats) while rats that were paired with an anesthetized demonstrator (n=7 rats) displayed significantly less freezing (main effect of treatment p=0.0038, $F_{(1,19)}$=15.15, eta^2=0.21;

treatment x trial interaction p=0.0013, F(12,228)=2.810, eta^2=0.043, two-way RM-ANOVA). Data shown here are mean ± 95% confidence intervals. #p<0.05, main effect of group in two-way RM-ANOVA; *p<0.05 two-tailed unpaired t-test.
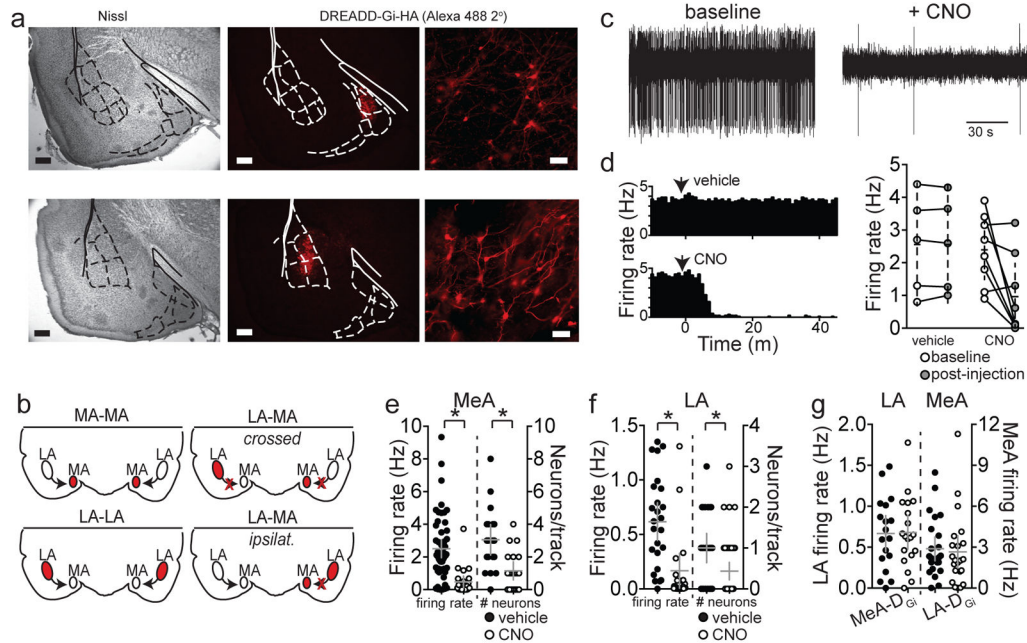
Figure 2. Electrophysiological verification of DREADD-Gi effect on MeA and LA neuron firing in vivo

The tissue from all rats was sectioned and stained for HA tag. **a)** Example photomicrographs (2X and 20X magnification) of immunostain for the HA tag of DREADD-Gi expression in MeA (top) and LA (bottom) and corresponding Nissl stained sections (left) to facilitate accurate identification of region. Overlay adapted from Paxinos and Watson[49]. **b)** Schematic representing the inactivation approaches including bilateral inactivation of MeA or LA, crossed inactivation of MeA and LA, or ipsilateral inactivation of MeA and LA. **c)** Neuronal firing rate and the number of spontaneously firing neurons per electrode track were quantified. This was followed by CNO or vehicle injection and the recording was repeated. All neuronal recording sites were verified histologically. Example of a MeA neuron firing under baseline conditions and another MeA neuron after CNO in the same rat. **d)** In some experiments a neuron was recorded during injection of vehicle or CNO, providing pre- and post-injection measures of the same neurons for with-in neuron comparisons. When recording site was verified to lie within DREADD expression area, 5/8 neurons displayed a >75% decrease in firing rate after CNO injection, but 0/5 displayed a decrease after vehicle. **e)** In the remaining recordings, firing of different neurons was sampled before and after CNO or vehicle injection, providing a between-neuron comparison. CNO injection in rats with DREADD-Gi in the MeA significantly decreased the overall firing rate (vehicle 2.50 ± 0.27 Hz, n=53 neurons from 4 rats, CNO 0.47 ± 0.17 Hz, n=23 neurons from 4 rats, p=0.001, t=3.41, df=74, eta^2=0.23, 95% C.I.=−2.9 to −1.2, two-tailed unpaired t-test) and number of spontaneously firing posterior MeA neurons compared to vehicle (vehicle 3.05 ± 0.44 neurons/track, n=19 tracks, CNO 1.15 ± 0.26 neurons/track, n=20 tracks, p=0.0006, t=3.736, df=37, eta^2=0.27, 95% C.I.=−2.93 to −0.87, two-tailed unpaired t-test). **f)** CNO injection in rats with DREADD-Gi in the LA decreased the overall firing rate (vehicle 0.62 ± 0.08 Hz, n=25 neurons from 3 rats, CNO 0.17 ± 0.08, n=20 neurons from 3 rats, p=0.0004, t=3.878, df=43, eta^2=0.26, 95% C.I.=−0.69 to −0.22, two-tailed unpaired t-test)

and number of spontaneously firing neurons in LA compared to vehicle (vehicle 1.00 ± 0.17 neurons/track, n=25 tracks, CNO 0.44 ± 0.11 neurons/track, n=46 tracks, p=0.0045, t=2.940, df=69, eta^2=0.11, 95% C.I.=-0.95 to -0.18, two-tailed unpaired t-test). **g)** In contrast, CNO did not significantly impact the firing rate of MeA neurons recorded from rats with DREADD-Gi in LA (vehicle 2.88 ± 0.42 Hz, n=25 neurons from 4 rats, CNO 2.66 ± 0.57Hz, n=22 neurons from 4 rats, p=0.745, t=0.328, df=45, eta^2=0.002, 95% C.I.=-1.2 to 1.6, two-tailed unpaired t-test), nor did it impact the firing rate of LA neurons from rats with DREADD-Gi in MeA (vehicle 0.67 ± 0.10 Hz, n=18 neurons from 4 rats, CNO 0.68 ± 0.10 Hz, n=19 neurons from 4 rats, p=0.934, t=0.084, df=35, eta^2=0.0002, 95% C.I.=-0.30 to -0.28, two-tailed unpaired t-test). Data shown here are mean $\pm$ 95% confidence intervals. Scale bars at 2X=500 μm, 20X=100 μm.
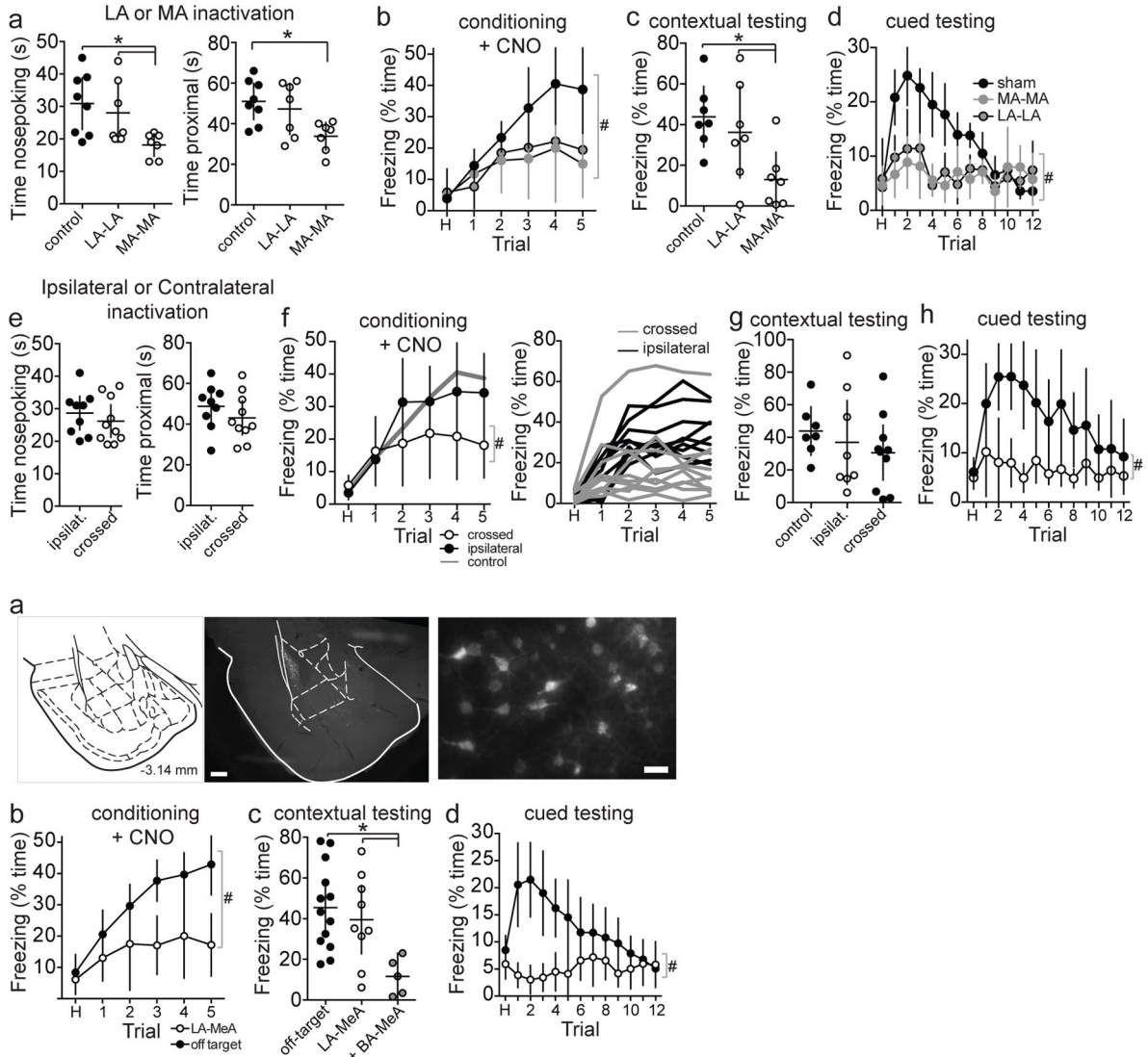
Figure 3. Disruption of intra-amygdala path impairs social fear learning

Bilateral inactivation of MeA (MA-MA) or LA (LA-LA), or unilateral inactivation of LA and MeA in contralateral hemispheres (LA-MA/crossed) or in the same hemisphere (LA-MA/ipsilat) was induced by CNO administration (1 mg/kg) 40 minutes prior to social fear conditioning. **a**) Control rats (n=8 rats) displayed social approach during social fear conditioning, measureable as time spent close to and nose exploring through the mesh divider. Bilateral inactivation of MeA (n=7 rats), but not LA (n=7 rats), decreased nose poking (p=0.02, $F_{(2,19)}$=4.74, eta^2=0.33, one-way ANOVA; *p<0.05 Holm-Sidak's multiple comparisons test). Similarly, bilateral inactivation of MeA (n=7 rats), but not LA (n=7 rats), decreased time proximal to the divider (p=0.0178, $F_{(2,19)}$=5.015, eta^2=0.35, one-way ANOVA; *p<0.05 Holm-Sidak's multiple comparisons test). **b**) Inactivation of MeA or LA decreased freezing during social fear conditioning (main effect of inactivation p=0.047, $F_{(2,19)}$=3.61, eta^2=0.11; trial x inactivation interaction p=0.0034, $F_{(10,95)}$=2.89, eta^2=0.07, two-way RM-ANOVA; #p<0.05, main effect of group in two-way RM-ANOVA). **c**)

Contextual freezing was measured after 48 hours in the same context as conditioning, without CNO. Bilateral inactivation of MeA (n=7 rats), but not LA (n=7 rats) during conditioning, decreased contextual freezing (p=0.018, F(2,19)=5.11, eta^2=0.36, one-way ANOVA; *p<0.05 Holm-Sidak's multiple comparisons test). **d**) Freezing to the CS+ tone was tested after 48 hours in a novel context, without CNO. Bilateral inactivation of MeA or LA during conditioning decreased freezing in response to the CS+ tone during testing (main effect of inactivation p<0.0001, F(2,19)=19.74, eta^2=0.18; trial x inactivation interaction p<0.0001, F(24,228)=6.01, eta^2=0.20, two-way RM-ANOVA; #p<0.05, main effect of group in two-way RM-ANOVA). **e**) Crossed functional disconnection of LA and MeA (n=10 rats) did not decrease social approach during social fear conditioning (p=0.447, t=0.778, df=17, eta^2=0.035, 95% C.I.=−4.2 to 9.2, two-tailed unpaired t-test) compared to ipsilateral inactivation of LA and MeA (n=9 rats). **f**) However, crossed functional disconnection of LA and MeA did decrease freezing to the CS+ during social fear conditioning (trial x inactivation interaction p=0.0027, F(5,85)=3.974, eta^2=0.047, two-way RM-ANOVA) shown in grouped data (left) and individual rats (right). **g**) Crossed functional disconnection of LA and MeA did not impair contextual fear (p=0.625, t=0.499, eta^2=0.015, 95% C.I.=−20.7 to 33.5, df=17, two-tailed unpaired t-test). **h**) But crossed functional disconnection of LA and MeA did impair freezing in response to the CS+ tone when measured in a novel context after 48 hours (main effect of inactivation p=0.0023, F(1,17)=12.88, eta^2=0.22; trial x inactivation interaction p=0.0003, F(12,204)=3.21, eta^2=0.061, two-way RM-ANOVA). **i**) DREADD-Gi was transduced in LA neurons that project to MeA by infusion of CAV2-Cre into MeA with a Cre-dependent DREADD-Gi vector in the LA. **j)** CNO was injected 40 minutes prior to social fear conditioning. Rats that had DREADD-Gi expression in LA-MeA neurons (n=9 rats) displayed reduced freezing during social fear learning compared to rats whose vector infusion was off-target (n=13 rats; main effect of inactivation site p=0.0001, F(1,20)=23.18, eta^2=0.15; trial x inactivation interaction p=0.0138, F(5,100)=3.026, eta^2=0.054, two-way RM-ANOVA). **k**) Contextual conditioned social fear was compared between rats with DREADD-Gi expression in the LA, LA+BA, and off-target expression. Contextual conditioned social fear was not impaired in rats with DREADD-Gi expression limited to LA-MeA neurons (n=9 rats) compared to rats whose vector infusion was off-target (n=13 rats; p=0.0116, F(2,24)=5.397, eta^2=0.31, one-way ANOVA; p>0.05 Holm-Sidak's multiple comparisons test), but was impaired when DREADD transduction extended to include LA and BA neurons (n=5 rats; p<0.05 Holm-Sidak's multiple comparisons test compared to off-target infusions and on-target infusions). **l**) Conditioned freezing to cue was significantly impaired in rats with DREADD-Gi expression in LA-MeA neurons (n=9 rats) compared to rats whose vector infusion was off-target (n=13 rats) measured in a novel context after 48 hours (main effect of inactivation site p<0.0001, F(1,20)=25.39, eta^2=0.16; trial x inactivation interaction p<0.0001, F(12,240)=4.168, eta^2=0.11, two-way RM-ANOVA). *p<0.05 Holm-Sidak's multiple comparisons test, #p<0.05, main effect of group in two-way RM-ANOVA. Scale bars at 2X=500 μm, 20X=50 μm. Data shown here are mean ± 95% confidence intervals.
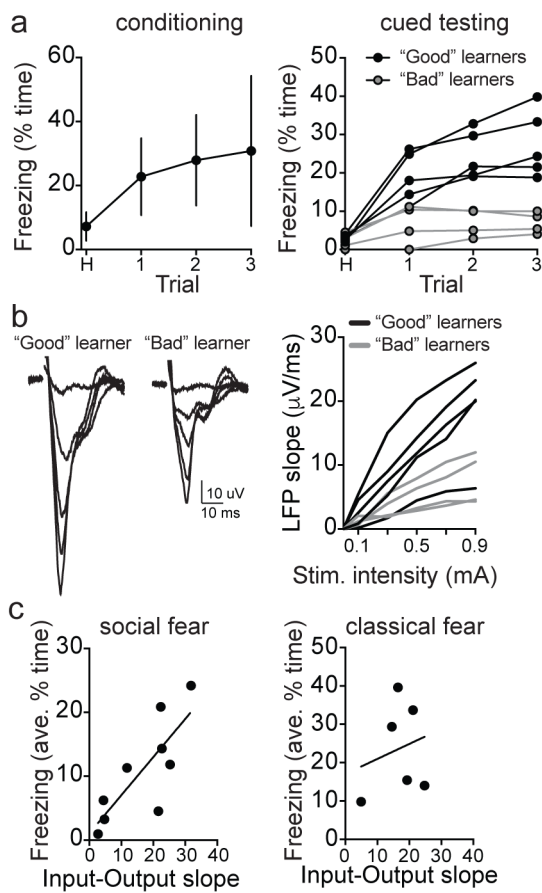
Figure 4. LA-MeA strength associated with social fear learning
a) A modified, weaker version of social fear conditioning (3 trial conditioning, left; n=9 rats) produces substantial variability between rats in conditioned freezing, with some rats displaying robust conditioned freezing ("Good" learners, n=5 rats) and others displaying minimal conditioned freezing ("Bad" learners, n=4 rats). **b**) Stimulation of LA caused a local field potential response in the posterior MeA, measured as the slope of the initial deflection. The slope was measured across a range of stimulation intensities to produce an input-output curve. "Good" learners tended to display a greater local field potential than "Bad" learners. **c**) The slope of the LA-MeA input-output curve was quantified as a measure of the strength of the LA-MeA local field potential. There was a significant correlation between the LA-MeA strength and social fear learning in individual rats (quantified as average percent time freezing during test; Pearson r = 0.78, R square = 0.64, p=0.01). In control experiments there was no correlation between LA-MeA strength and classical fear conditioning in individual rats (n=6 rats, Pearson r = 0.22, R square = 0.049, p=0.67). Data shown here are mean ± 95% confidence intervals except where noted.
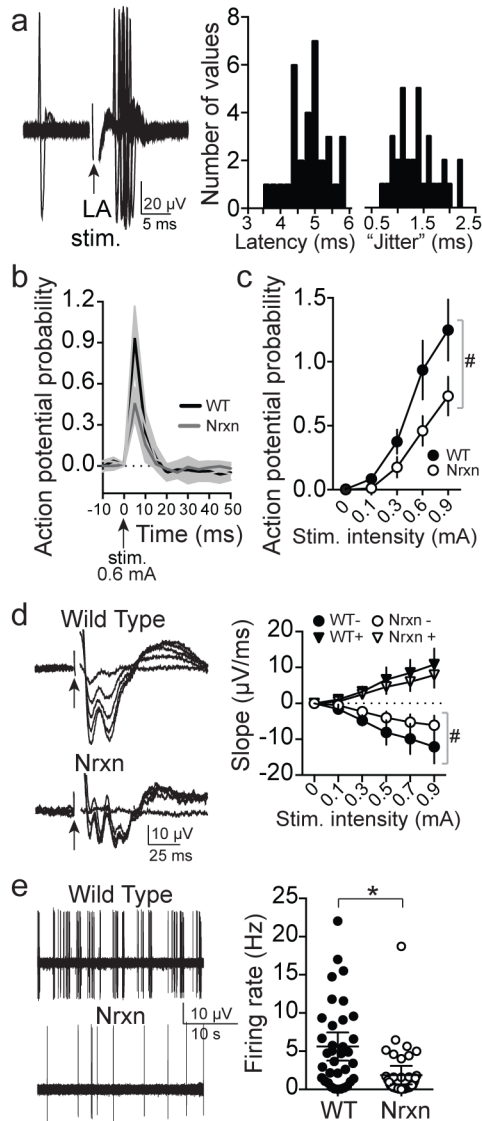
Figure 5. Disruption of intra-amygdala path in neurexin knock-out rats

a) Stimulation of LA caused increased firing in posterior MeA neurons *in vivo* (n=16 neurons from 5 rats, defined as >3 times baseline firing rate in a 5 ms time window within 10 ms of LA stimulation). Responses were included in analysis only if they met criteria for monosynaptic connections (average latency 4.9 ms, range 3.7 – 5.8 ms, latency jitter average 1.37 ms, range 0.66 – 2.21 ms. Shown here are frequency histograms of the distribution of latency and latency jitter). **b**) The average response was significantly weaker in Nrxn rats at the same stimulation intensity (WT n=16 neurons from 5 rats, Nrxn n=11 neurons from 5 rats, 0.6 mA, mean ± 95% confidence interval; genotype x time interaction p<0.0001, $F(78,1950)=2.744$, $eta^2=0.053$, two-way RM-ANOVA). **c**) The response of these same MeA neurons was significantly weaker in Nrxn rats over a range of LA stimulation intensities (main effect of genotype p<0.0001, $F(1,125)=35.94$, $eta^2=0.070$; genotype x stimulation interaction p=0.0002, $F(4,125)=6.05$, $eta^2=0.047$, two-way RM-ANOVA). **d**) The field potential in posterior MeA evoked by LA stimulation was significantly reduced in Nrxn rats

(n=16 rats) compared to WT (n=11 rats; slope of the 1st negative peak; main effect of genotype on negative peak p=0.011, $F_{(1,25)}=7.50$, eta^2=0.087; genotype by stimulation intensity interaction p=0.0043, $F_{(4,100)}=4.06$, eta^2=0.041, two-way RM-ANOVA). **e)** The firing rate of posterior MeA neurons *in vivo* was significantly decreased in Nrxn compared to WT rats (WT 5.6 ± 0.9 Hz, n=36 neurons from 8 rats, Nrxn 1.9 ± 0.6 neurons, n=59 neurons from 9 rats, p=0.0005, t=3.583, df=93, eta^2=0.12, 95% C.I.=−5.82 to −1.67, two-tailed unpaired t-test). Data shown here are mean ± 95% confidence intervals except where noted.
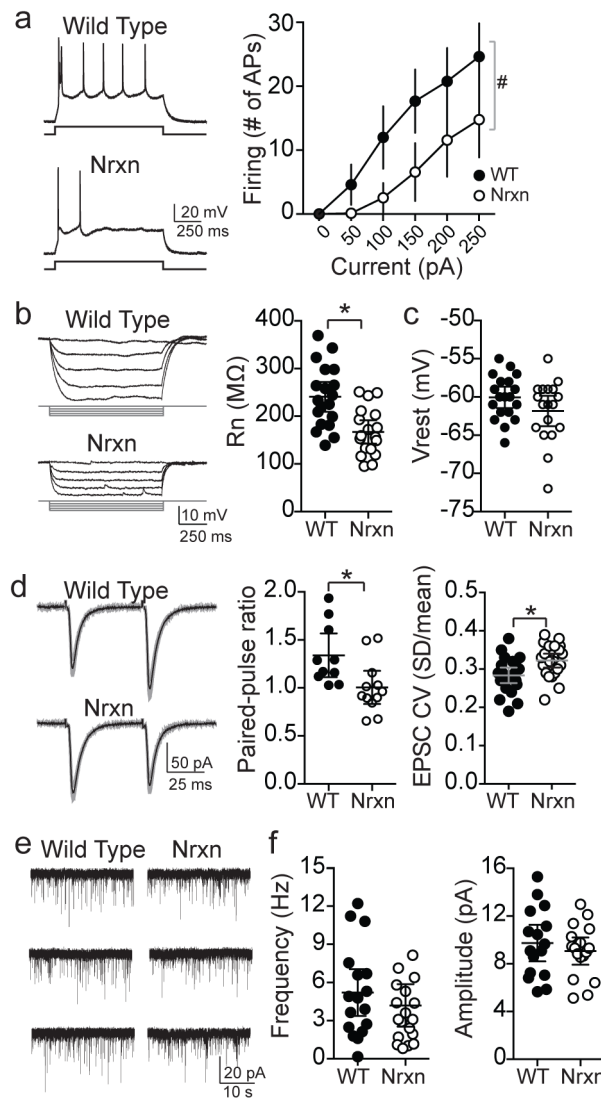
Figure 6. Intrinsic and synaptic properties of MeA neurons

Properties of MeA (posterior) neurons were measured in vitro using whole cell recordings. **a)** Posterior MeA neurons (Type I neurons based on firing pattern[50, 51]) recorded in vitro from Nrxn rats had significantly lower membrane excitability compared to WT (WT n=11 neurons from 11 slices, Nrxn n=12 neurons from 12 slices, main effect of genotype, p=0.0004, $F_{(1,21)}$ = 17.6, eta^2=0.21; genotype x current interaction p<0.001, $F_{(4,84)}$=18.8, eta^2=0.15, two-way RM ANOVA). **b)** MeA neurons from Nrxn rats displayed significantly lower input resistance than WT (p=0.0004, t=3.875, df=35, eta^2=0.30, 95% C.I.=−112.2 to −35.1, two-tailed unpaired t-test, WT n=19 neurons from 14 slices, Nrxn n=18 neurons from 13 slices). **c)** The resting membrane potential of these same MeA neurons was not significantly different between WT and Nrxn rats (p=0.129, t=1.556, df=35, eta^2=0.065, 95% C.I.=−4.10 to 0.54, two-tailed unpaired t-test, WT n=19 neurons, Nrxn n=18 neurons). **d)** Paired-pulse facilitation and coefficient of variance (CV) of EPSCs evoked by local stimulation was measured to assess synaptic function. The paired-pulse ratio of EPSCs in

MeA neurons was significantly less in Nrxn rats (WT=10 neurons from 10 slices, Nrxn=12 neurons from 12 slices, p=0.015, t=2.66, df=20, eta^2=0.26, 95% C.I.=−0.60 to −0.07, two-tailed unpaired t-test). CV of EPSCs in MeA neurons was significantly higher in Nrxn rats (WT=22 neurons, Nrxn=23 neurons, p=0.0049, t=2.965, df=43, eta^2=0.17, 95% C.I.=0.012 to 0.065, two-tailed unpaired t-test). **e)** Miniature EPSCs (mEPSCs) were recorded from MeA neurons (WT n=17 neurons from 14 slices, Nrxn n=19 neurons from 14 slices). **f)** The mEPSC frequency (left; p=0.397, t=0.859, df=34, two-tailed unpaired t-test) and amplitude (right; p=0.457, t=0.753, eta^2=0.021, 95% C.I.=−3.39 to 1.38, two-tailed unpaired t-test) were not significantly different between WT and Nrxn rats. *p<0.05 two-tailed unpaired t-test, #p<0.05, main effect of group in two-way RM-ANOVA. Data shown here are mean ± 95% confidence intervals.
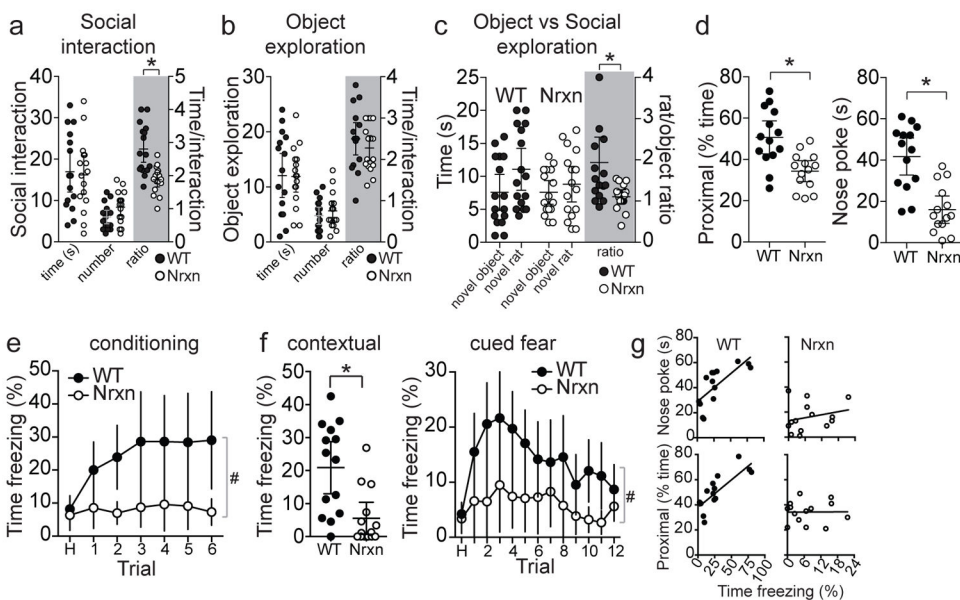
Figure 7. Social learning is impaired in neurexin rats

a) Social interaction with a novel rat in the open field was measured from WT and Nrxn rats (n=16 rats/group). There was no significant difference in the total time of interaction (p=0.814, t=0.238, df=30, eta^2=0.002, 95% C.I.=−7.19 to 5.69, two-tailed unpaired t-test) or the number of interaction events (p=0.066, t=1.908, df=30, eta^2=0.11, 95% C.I.=−0.17 to 4.92, two-tailed unpaired t-test). However, the duration of individual interaction events was significantly lower in Nrxn rats (p=0.0001, t=4.382, df=30, eta^2=0.39, 95% C.I.=−1.36 to −0.50, two-tailed unpaired t-test). **b**) Novel object exploration was measured in the open field (n=16 rats/group). There was no significant difference between WT and Nrxn rats in the total time of object exploration (p=0.936, t=0.082, df=30, eta^2=0.0002, 95% C.I.=−4.88 to 4.51, two-tailed unpaired t-test), the number of exploration events (p=0.428, t=0.803, df=30, eta^2=0.021, 95% C.I.=−1.35 to 3.10, two-tailed unpaired t-test), nor the duration of each object exploration event (p=0.330, t=0.990, df=30, eta^2=0.032, 95% C.I.=−0.35 to 0.12, two-tailed unpaired t-test). **c**) WT and Nrxn rats both display a preference for a novel rat when novel rat and novel object are presented together (n=16/group; object vs novel rat stimulus main effect, p<0.0001, F(1,30)=32.82, eta^2=0.056, two-way RM-ANOVA). However, WT rats display a significantly greater preference for a novel rat than Nrxn rats display (stimulus x genotype interaction, p=0.011, F(1,30)=7.364, eta^2=0.013; novel rat/object preference ratio, p=0.009, t=2.774, df=30, eta^2=0.20, 95% C.I.=−1.44 to −0.22, two-tailed unpaired t-test). **d**) Social fear conditioning was measured in WT and Nrxn rats (n=14 rats/group). Nrxn rats displayed significantly less time proximal to the divider (left; time proximal to divider p=0.0001, t=3.78, df=26, eta^2=0.35, 95% C.I.=−25.4 to −7.4, two-tailed unpaired t-test) and less time nose exploring through the divider (right; p<0.0001, t=5.00, df=26, eta^2=0.49, 95% C.I.=−36.3 to −15.1, two-tailed unpaired t-test). **e**) These same Nrxn rats displayed significantly less freezing during social fear conditioning (main effect of genotype, p=0.0043, F(1,26)=9.790, eta^2=0.18; genotype x trial interaction, p=0.0081, F(6,156)=3.015, eta^2=0.030, two-way RM-ANOVA, n=14 rats/group). **f**) When tested after 48 hours, these Nrxn rats displayed significantly less contextual freezing in the conditioning

context (left; p=0.0014, t=3.579, df=26, eta^2=0.33, 95% C.I.=−24.2 to −6.5, two-tailed unpaired t-test) and cued freezing in a novel context (right; main effect of genotype, p=0.0088, F(1,26)=8.022, eta^2=0.126, two-way RM-ANOVA, n=14 rats/group). **g**) Freezing behavior on the testing day was correlated with social approach behaviors on conditioning day in WT rats, but not in Nrxn rats (shown here are individual values, n=14 rats/group). WT rats that spent more time close to the mesh divider during social fear conditioning, and spent more time nose exploring through the divider displayed greater conditioned social fear (proximal to divider r^2=0.65, p<0.01; nose poking r^2=0.54, p<0.01). The correlation between these pro-social behavioral measures and fear learning were absent in Nrxn rats (proximal to divider r^2=0.01, p>0.05; nose poking r^2=0.10, p>0.05). Data shown here are mean ± 95% confidence intervals except where noted noted. *p<0.05 two-tailed unpaired t-test, #p<0.05, main effect of group in two-way RM-ANOVA.
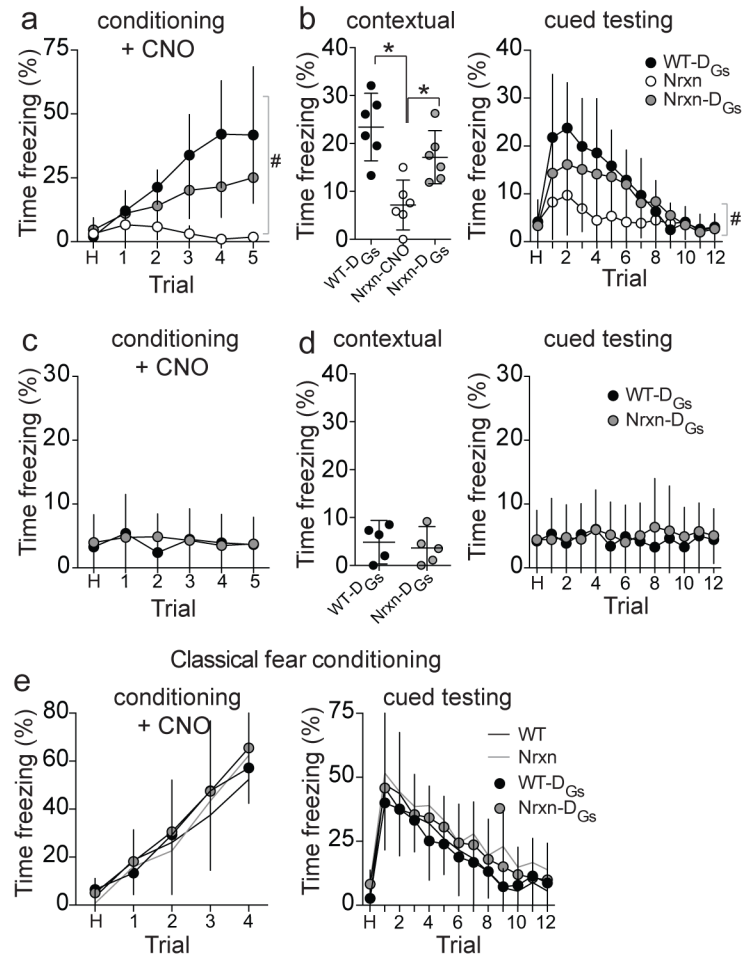
Figure 8. DREADD-Gs activation of MeA partially rescues social learning deficits in neurexin rats

DREADD-Gs expression was transduced to activate posterior MeA. Control rats had reported only transduced. CNO (1 mg/kg i.p.) was administered 40 minutes prior to social fear conditioning. **a**) Activation of MeA partially restored freezing during social fear conditioning in Nrxn rats (n=6 rats) to WT levels (n=5 rats), and better than control Nrxn rats without MeA activation (n=6 rats; main effect of treatment, $p<0.0001$, $F_{(2,14)}=19.90$, $eta^2=0.344$; treatment x trial interaction, $p<0.0001$, $F_{(10,70)}=8.11$, $eta^2=0.190$ two-way RM-ANOVA). **b**) When tested after 48 hours, control Nrxn rats displayed impaired freezing to the context compared to WT rats ($p=0.0007$, $F_{(2,15)}=12.44$. $eta^2=0.624$, one-way ANOVA between WT-DREADD-Gs, control Nrxn and Nrxn-DREADD-Gs, $p<0.05$ Holm-Sidak's multiple comparisons test) while Nrxn rats that had MeA activation (DREADD-Gs) during social fear conditioning displayed significantly enhanced contextual freezing to the conditioned context compared to control Nrxn rats ($p<0.05$ Holm-Sidak's multiple comparisons test). These same Nrxn DREADD-Gs rats also displayed significantly enhanced conditioned freezing to the CS+ in a novel context, compared to control Nrxn rats (main effect of treatment, $p<0.0097$, $F_{(2,14)}=6.58$, $eta^2=0.117$; treatment x trial interaction, $p<0.0001$, $F_{(24,168)}=3.098$, $eta^2=0.116$, two-way RM-ANOVA). **c**) To verify that

DREADD-Gs activation of the MeA did not induce spurious freezing unrelated to social learning, social fear conditioning experiments were repeated with MeA activation (CNO, 1 mg/kg, i.p.) using a demonstrator that was anesthetized (as above). Neither WT-DREADD-Gs rats (n=5 rats) nor Nrxn-DREADD-Gs rats (n=5 rats) displayed freezing during conditioning if the demonstrator was anesthetized (main effect of trial, p=0.861, $F_{(5,40)}$=0.379, eta^2=0.027; main effect of genotype, p=0.816, $F_{(1,8)}$=0.0577, eta^2=0.0027; genotype x trial interaction, p=0.881, $F_{(5,40)}$=0.347, eta^2=0.025, two-way RM-ANOVA). **d)** There was also no conditioned freezing displayed by these rats in response to the context (p=0.620, t=0.516, df=8, eta^2=0.032, 95% C.I.=−6.46 to 4.10, two-tailed unpaired t-test) or tone (in a novel context; main effect of trial, p=0.996, $F_{(12,96)}$=0.235, eta^2=0.019; main effect of genotype, p=0.661, $F_{(1,8)}$=0.207, eta^2=0.0078; genotype x trial interaction, p=0.991, $F_{(12,96)}$=0.285, eta^2=0.023) measured after 48 hours. **e)** Activation of MeA during classical fear conditioning (WT n=7, Nrxn n=6, WT-DREADD-Gs n=6, Nrxn-DREADD-Gs n=6) did not significantly impact freezing during conditioning (main effect of group, p=0.315, $F_{(3,21)}$=0.641, eta^2=0.0082; group x trial interaction, p=0.929, $F_{(12,84)}$=0.465, eta^2=0.014, two-way RM-ANOVA), nor conditioned freezing during testing after 48 hours (main effect of group, p=0.315, $F_{(3,21)}$=1.255, eta^2=0.033; group x trial interaction, p=0.999, $F_{(36, 252)}$=0.369, eta^2=0.013, two-way RM-ANOVA). Data shown here are mean ± 95% confidence intervals. p<0.05 post-hoc Holm-Sidak comparison after ANOVA, #p<0.05, main effect of group in two-way RM-ANOVA.